2.5. Analysis of apoptosis and caspase activities

To quantify apoptosis, cells were labeled with fluorescein isothiocyanate (FITC)-conjugated Annexin V (BD Biosciences, Palo Alto, CA), then subjected to flow cytometric analysis. For analysis of nuclear DNA fragmentation, the terminal deoxynucleotidyl transferase (TdT)-mediated dUTP nick end-labeling (TUNEL) assay was done according to the manufacturer's recommendations (DeadEnd Fluorometric TUNEL Systems; Promega). Cells were analyzed using a FACS Calibur flow cytometer (BD Biociences) and fluorescence microscopy. Activities of caspase-3, -8, and -9 were determined by using green fluorochrome-labeled inhibitors of caspases (FLICA)-3, -8, and -9 (FLICA Apoptosis Detection Kit; Immunochemistry Technologies, Bloomington, MN). Cells from LCLs were treated with 10 μg/ml of DHMEQ (+) or with DMSO alone (−) for 8 h and fixed on slides; active caspases were detected by FLICA-3, -8, and -9. For detection of nuclear DNA, cells were stained with Hoechst 33342 and photographed through a UV filter and an Olympus BX50F microscope (Olympus, Tokyo, Japan).

2.6. In vivo effects of DHMEQ on NOG mice inoculated with LCLs

NOG mice were purchased from the Central Institute for Experimental Animals (Kawasaki, Japan). The Ethical Review

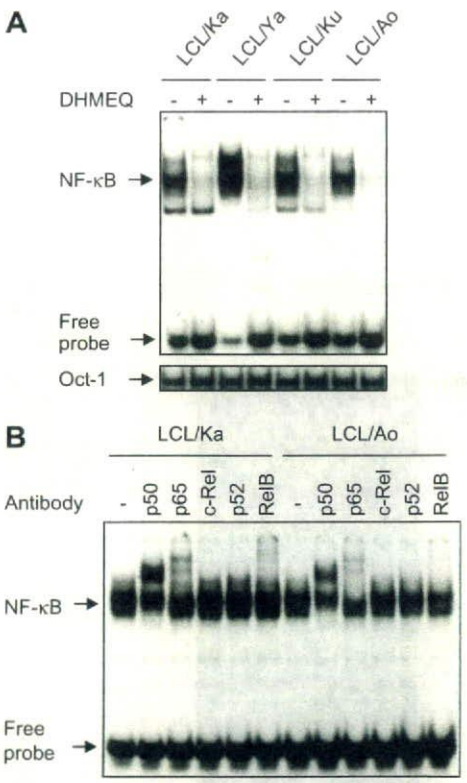

Fig. 1. Inhibition of constitutive NF-κB binding activity in LCLs by DHMEQ. (A) Inhibition of constitutive NF-κB activity in LCLs. LCLs were treated with 10 μg/ml of DHMEQ (+) or with DMSO alone (−) for 3 h. Nuclear extracts (2.5 μg) were examined for NF-κB binding activity by electrophoretic mobility shift analysis (EMSA) with a radiolabeled NF-κB-specific probe. Binding of Oct-1 served as a control. (B) Subcomponents of constitutive NF-κB activity in LCLs. Nuclear extracts (1 μg) of cells without DHMEQ treatment were subjected to supershift analysis with antibodies specific for NF-κB p50, p65, c-Rel, p52, and RelB or without antibody (−). The experiment using isotype matched IgG control showed the same result (data not shown). The position of shifted bands corresponding to NF-κB and free probes are indicated on the left.

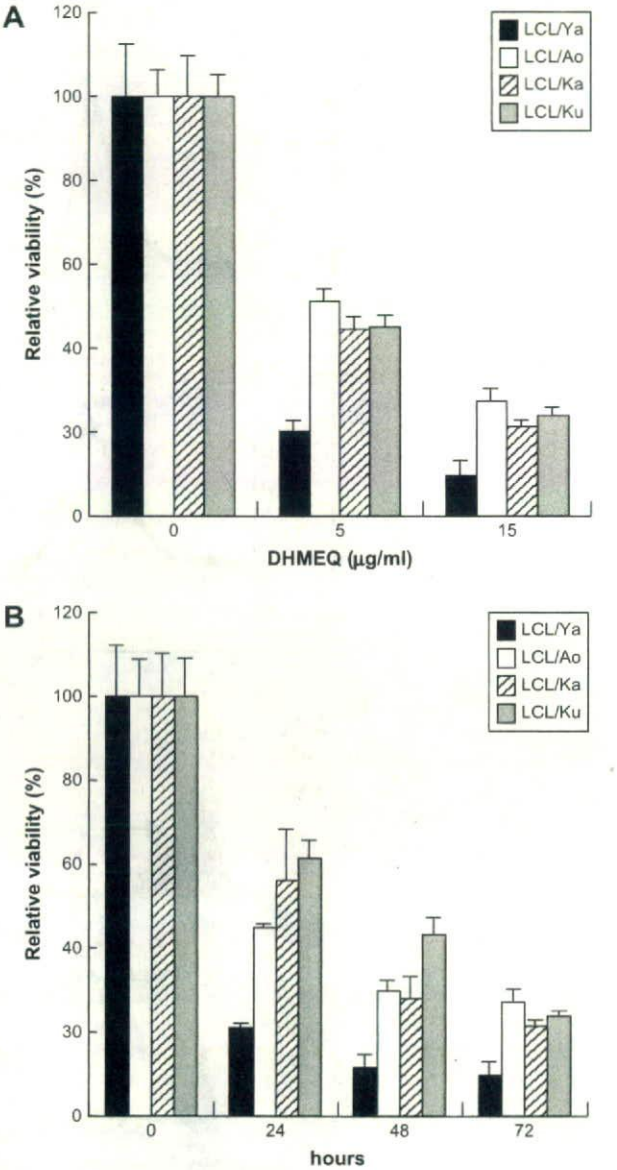

Fig. 2. DHMEQ inhibits proliferation of LCLs. The viability of the cells was determined by WST-8 assay and the relative levels compared with those of DMSO-treated cells are presented. Data represent the mean and standard deviation of triplicate experiments. (A) Results of dose–response experiments. LCLs were treated with 0, 5, or 10 μg/ml of DHMEQ for 72 h. ALL LCLs treated with 0, 5, or 10 μg/ml of DHMEQ showed statistical significance compared to DMSO-treated controls. (B) Results of time–response experiments. LCLs were treated with 10 μg/ml of DHMEQ for 24, 48, and 72 h. ALL LCLs treated for 24, 48, and 72 h except for LCL/Ku at the point of 24 h showed statistical significance compared to DMSO-treated controls.

Committee of the National Institute of Infectious Diseases approved the experimental protocol. 1×10^6 LCL cells were inoculated subcutaneously into the post-auricular region of NOG mice. DHMEQ was administered three times a week for 1 month into the post-auricular region of mice at a dose of 12 mg/kg, beginning on day 5 when tumors were palpable. The control mice were injected RPMI-1640 as was performed in our recent published papers [15,16]. Mice were killed 1 month after inoculation.

2.7. Immunohistochemistry

Cells were immunostained with antibodies and fluorescence signals were detected using confocal microscopy. Cytospin samples were prepared using 5×10^5 cells and cells were first washed three times with phosphate-buffered saline (PBS). Cells were then fixed with 100% cold acetone for 10 min at room temperature and washed three times in PBS. Samples were incubated with primary antibody at the concentration

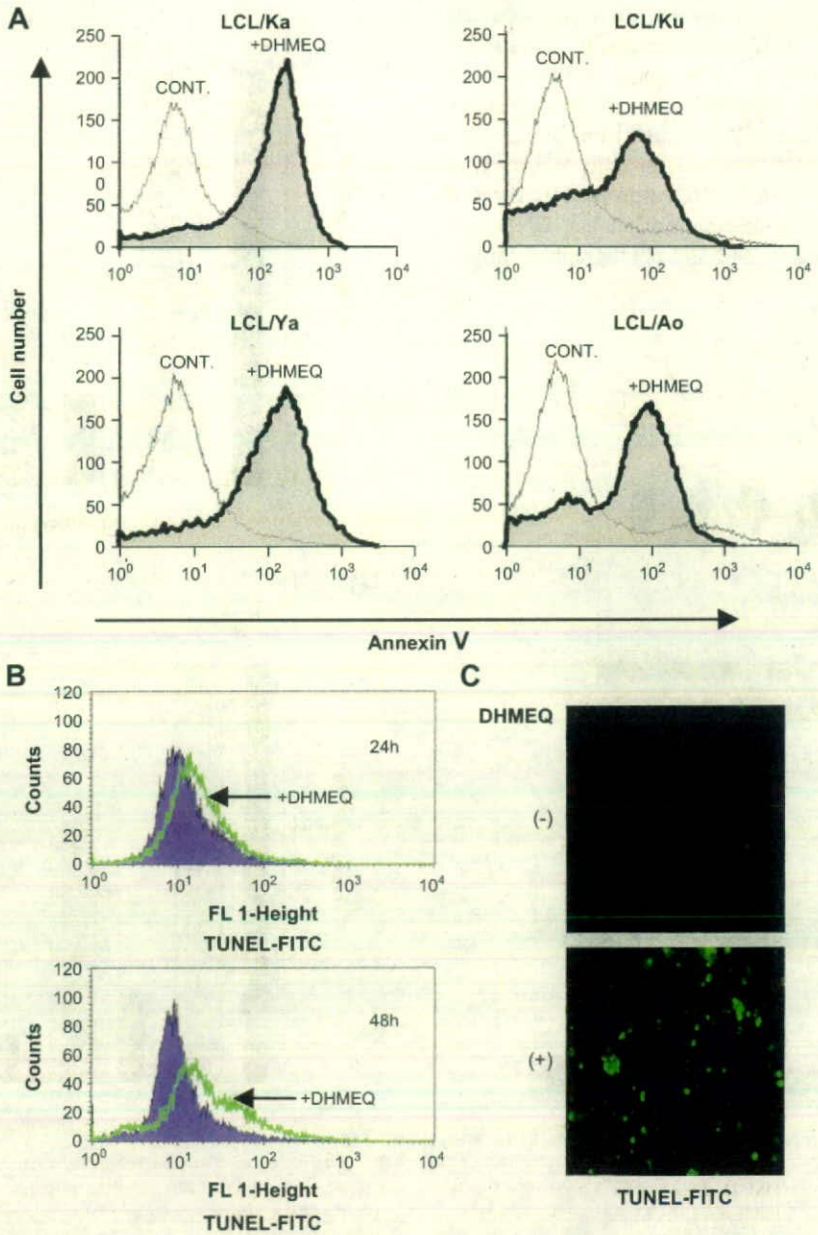

Fig. 3. DHMEQ induces apoptosis in LCLs. (A) Annexin V reactivity in LCLs after DHMEQ treatment. LCLs were treated with (filled curve) or without (open curve) 10 μg/ml of DHMEQ for 48 h, and the binding of FITC-conjugated Annexin V was analyzed by flow cytometry. (B) DNA fragmentation in LCL cells after DHMEQ treatment. DNA fragmentation in LCL cells was detected by TUNEL assay with flow cytometry. Representative flow cytometric profiles are shown for cells treated with 10 μg/ml of DHMEQ (open curve) or with DMSO alone (filled curve) for 24 h (upper panel) or 48 h (lower panel). (C) LCL cells were treated with 10 μg/ml of DHMEQ (+) or with DMSO alone (−) for 48 h, fixed on slides, and processed for TUNEL assay. A filter that selectively detects fluorescein isothiocyanate (FITC)-TUNEL fluorescence was used for the microscopic observation.

of 5 μg/ml at 4 °C overnight and washed with PBS three times. After incubation with fluorescence-labeled secondary antibody for 30 min at 37 °C, samples were washed three times in PBS and covered with a Perma Fluoro antifade reagent (Therme Shandon Co., Pittsburgh, PA). Fluorescence signals were detected using confocal microscopy (Radiance 2000) (Bio-Rad Laboratories. Antibodies used were as follows: anti-Epstein–Barr virus LMP clones CS, 1-4 mouse monoclonal antibody (Dako, Kyoto, Japan), and anti-p65 (c-20) goat polyclonal antibody (Santa Cruz Biotechnology Inc.

2.8. Real-time quantitative PCR

The expression level of anti-apoptotic genes was quantified by real-time reverse transcription–polymerase chain reaction (RT–PCR). Total RNA was extracted from the cells by ISOGEN reagent (Nippon Gene Co., Toyama, Japan) and treated according to the manufacturer's instructions. cDNA was synthesized using oligo dT and random primers synthesized with a PrimeScript RT reagent kit (Takara Bio Inc., Shiga, Japan). Amplification was performed with SYBR premix Ex Taq (Takara Bio Inc.) and the primer sets for c-IAP1, Bfl-1, BCL-XL, and c-FLIP (Takara Bio Inc.). The viral DNA load in EBV-infected PBMC was determined by real-time PCR with slight modifications of a previously described method [17]. DNA samples were extracted from the cells with a DNeasy tissue kit (Qiagen, Hilden, Germany). Amplification with SYBR premix Ex Taq (Takara Bio Inc.) and primers for BALF5 gene encoding the viral DNA polymerase (5′-CGG AAG CCC TCT GGA CTT C-3′ and 5′-CCC TGT TTA TCC GAT GGA ATG-3′) was performed using the Thermal Cycler Dice Real Time System (Takara Bio Inc.) and analyzed using the manufacturer's software.

2.9. Statistical analysis

Differences between mean values were assessed by *t*-test. A *P*-value of <0.05 was considered to be statistically significant.

3. Results

3.1. DHMEQ efficiently blocks constitutive NF-κB activity in LCLs

We first examined the effects of DHMEQ against constitutive NF-κB activity in established LCLs. Treatment with DHMEQ at a concentration of 10 μg/ml abrogated constitutive NF-κB binding activity in these cell lines (Fig. 1A). Components of NF-κB that are constitutively activated in LCLs were analyzed by

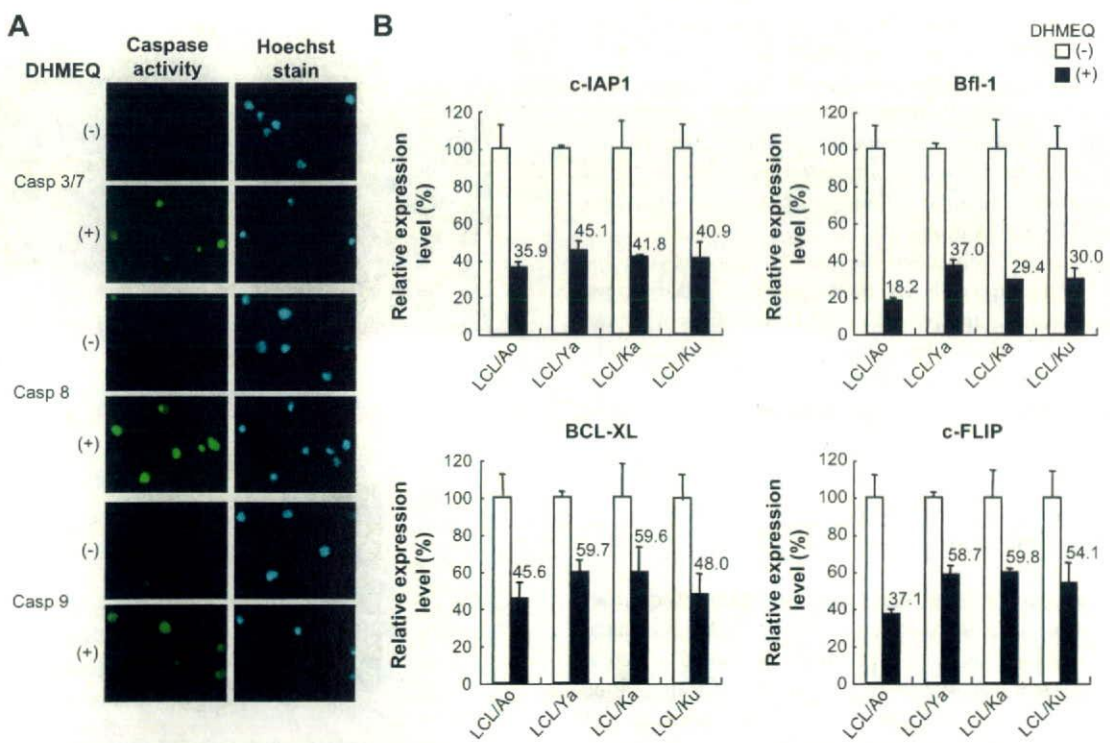

Fig. 4. Activation of caspase-3, -8, and -9. (A) LCL cells were treated with 10 μg/ml of DHMEQ (+) or with DMSO alone (−) for 8 h and fixed on slides. Caspase-3/7, -8, and -9 activities in LCLs after DHMEQ treatment were detected by green fluorochrome-labeled inhibitors of caspases (FLICA)-3/7, -8, and -9 (left panels) and nuclear DNA was stained with Hoechst 33342 (right panels). (B) Effects of DHMEQ on genes regulating apoptosis in LCLs. Quantification of the gene expression by real-time PCR. LCLs were treated with 10 μg/ml of DHMEQ (+) or with DMSO alone (−) for 4 h. The expressions of c-IAP1, Bfl-1, BCL-XL, and c-FLIP were quantified by real-time PCR. The data are means with standard deviation of triplicate experiments. The numbers above the bar graphs indicate the means of each gene expression after DHMEQ treatment. The reduction of the expressions of c-IAP1, Bfl-1, BCL-XL, and c-FLIP was statistically significant.

supershift assays. The results revealed that the NF-κB components consist of p50, p65, and RelB (Fig. 1B).

3.2. DHMEQ induces apoptosis of LCLs

To study the significance of NF-κB activation in the growth of LCLs, we examined the effects of DHMEQ on cell viability. Results of WST-8 assays showed that DHMEQ treatment reduced the cell viability of all four LCLs in a dose- and time-dependent manner (Fig. 2A and B).

NF-κB plays a key role in resistance to apoptosis [18]. Thus, we next examined whether DHMEQ induces apoptosis of LCLs by analyzing Annexin V reactivity and DNA fragmentation. Flow cytometric analysis showed a significant increase in the number of Annexin V-positive cells after DHMEQ treatment (Fig. 3A). Fragmentation of the nuclei of LCLs was clearly demonstrated after DHMEQ treatment by the TUNEL assay (Fig. 3B and C).

3.3. DHMEQ-induced apoptosis involves activation of caspases 3, 8, and 9

To confirm that the induction of apoptosis in LCLs by DHMEQ is caused by activation of the caspase pathway, we first examined activation of caspase-3/7 by immunostaining, using an antibody that recognizes a cleaved form of caspase-3/7. Results clearly showed cleavage of caspase-3/7, confirming that DHMEQ-induced apoptosis is associated with activation of the caspase pathway (Fig. 4A, top). To differentiate the membranous and mitochondrial pathways, we next examined the activation of caspases 8 and 9, which are upstream of caspase-3/7, by immunostaining. DHMEQ-treated LCL cells showed activation of both caspase-8 and caspase-9 (Fig. 4A, middle and bottom).

To understand the molecular mechanisms of apoptosis induction of LCLs after NF-κB inhibition by DHMEQ, we next examined by quantitative RT–PCR the changes in the expression levels of anti-apoptotic genes c-IAP1, Bfl-1, Bcl-XL, and c-FLIP, reportedly under the control of NF-κB, after DHMEQ treatment. The results demonstrated down-regulation of all of these genes (Fig. 4B).

3.4. DHMEQ shows a potent inhibitory effect on the growth of LCL cells in NOG mice

Because results *in vitro* suggested potential efficacy of DHMEQ for the treatment of patients with EBV-associated lymphoproliferative diseases, we next examined whether DHMEQ treatment can suppress the growth of xenografted LCL cells in a NOG mouse model. The gross appearance of resected tumors in mice treated with DHMEQ showed reduction of the tumor mass 1 month after inoculation of LCL cells (Fig. 5A and B). A decrease in the size of tumors in mice treated with DHMEQ was demonstrated when compared with controls 1 month after the injection of LCL cells (Fig. 5C).

3.5. DHMEQ inhibits outgrowth of EBV-infected peripheral blood B-lymphocytes

EBV-infected B lymphocytes under immunocompromised conditions acquire latency III infection, which may lead to proliferation and transformation into lymphoproliferative diseases including lymphomas [2,3]. Previous data link NF-κB activation by LMP-1 to transformation; however, they also indicate that NF-κB activation is not sufficient for transformation and should coordinate with other signals like mitogen-activated protein kinases [19]. Roles of NF-κB activity in EBV-infected lymphocytes for their survival during the early phase of infection are not fully understood. Therefore, to investigate the roles of NF-κB activation on the survival of EBV-infected lymphocytes during the early phase of infection, we examined the effect of NF-κB inhibition by DHMEQ on their survival and the EBV viral load in PBMC infected with EBV. Lymphocytes infected with EBV under immunosuppressive conditions already show constitutive NF-κB activation as well as LMP1 expression. Treatment of these cells with DHMEQ inhibited translocation of NF-κB into the nucleus (Fig. 6A). DHMEQ treatment also eliminated LMP1-expressing lymphocytes from PBMC (Fig. 6B). Finally, DHMEQ treatment prevented the outgrowth of lymphocytes infected

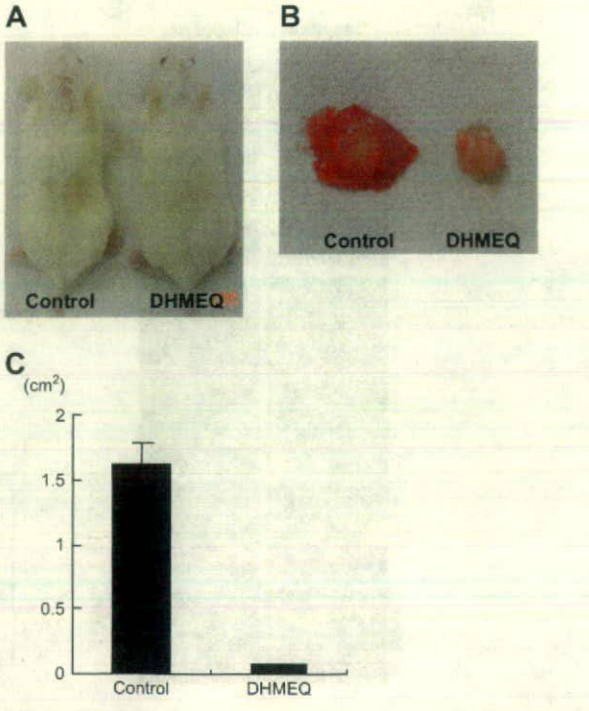

Fig. 5. DHMEQ inhibited the tumor growth of LCL cells *in vivo*. NOG mice were inoculated with LCL cells and administered DHMEQ (12 mg/kg) ($n = 5$) or control medium ($n = 5$) subcutaneously in the post-auricular region three times a week for up to 1 month. (A) Photograph of the backs of mice. (B) Photograph of a tumor at the site of LCL cells inoculation. (C) Subcutaneous tumor volume of mice inoculated with LCL cells and administered DHMEQ or control medium 1 month after inoculation.

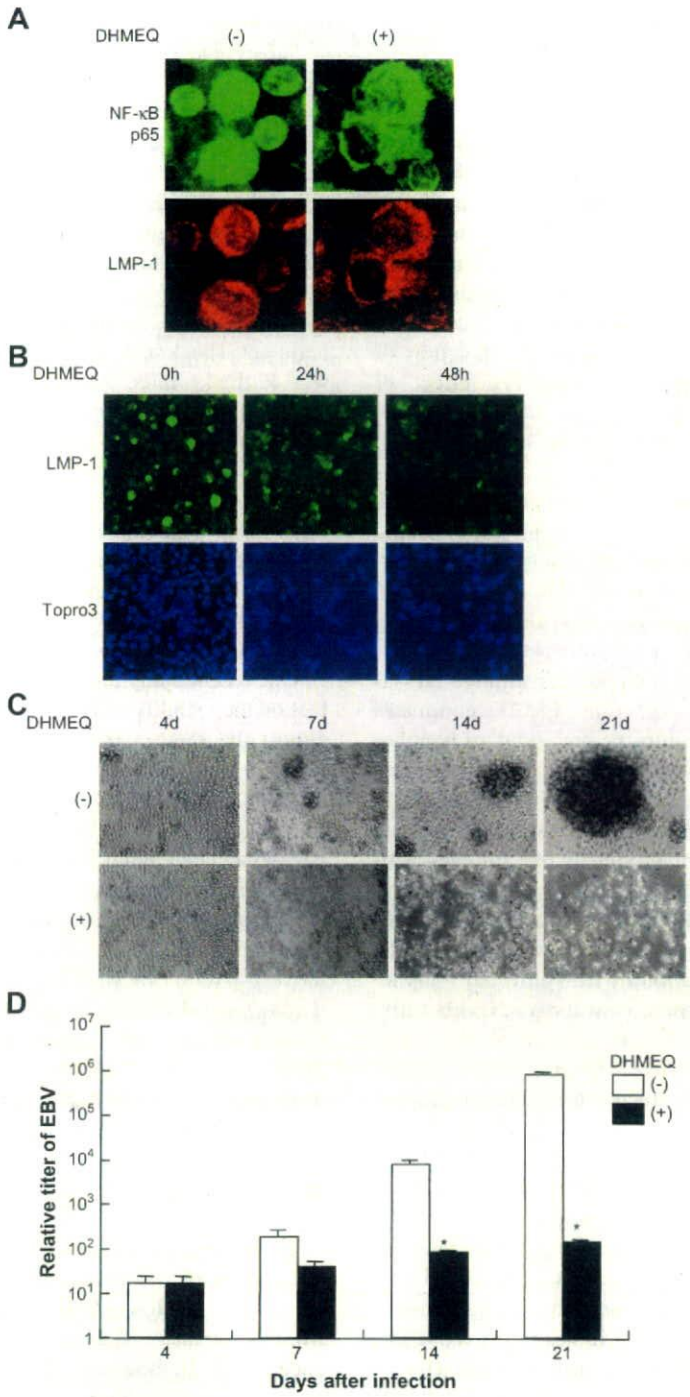

Fig. 6. Effects of DHMEQ on PBMC infected with EBV. 8×10^5/ml of PBMC from a healthy donor infected with EBV using supernatant of B95.8 line were cultured in RPMI 1640 medium supplemented with 10% FBS and 200 ng/ml cyclosporine A. Cells were harvested 4 days and 14 days after infection and served for experiments. (A) Inhibition of NF-κB and expression of LMP1 in lymphocytes. At the point of 4 days after infection, cells were treated with or without 10 μg/ml of DHMEQ for 1 h and immunostained with antibodies for LMP1 and NF-κB p65. DMSO-treated cells served as a control. (B) DHMEQ treatment eliminated LMP1 expressing cells from PBMC. At the point of 14 days after infection, cells were treated with or without 10 μg/ml DHMEQ for the indicated number of hours. Cells stained with anti-LMP1 antibody and topro 3 were observed by confocal microscopy. DMSO-treated cells served as a control. (C, D) Photographs of EBV-infected PBMC and quantification of viral load by real-time PCR. Cells cultured for 4 days were treated with 10 μg/ml of DHMEQ (+) or with DMSO alone (−) thereafter twice a week. Cells were observed by microscopy at the indicated days (C). Cells were harvested on the indicated days and genomic DNA was isolated. The viral load was quantified by real-time PCR as described in Section 2. The data are means and standard deviations of triplicate experiments (D). The asterisks indicate statistical significance.

with EBV and decreased the EBV viral load in PBMC (Fig. 6C and D).

4. Discussion

In the present study, we showed that the NF-κB inhibitor DHMEQ blocked strong and constitutive NF-κB activity, reduced viability, and induced apoptosis in LCLs. Induction of apoptosis by DHMEQ in LCLs is associated with inhibition of NF-κB, which is followed by down-regulation of NF-κB regulated anti-apoptotic genes. These observations, combined with our previous study about the mechanisms of action of DHMEQ [11], indicate that apoptosis induction of LCLs by DHMEQ is mediated by inhibitory effect of DHMEQ against NF-κB. DHMEQ appears to be more specific to NF-κB pathway compared with IκB kinase (IKK) inhibitor, Bay 11-7082 used in the previous studies [20,21], because DHMEQ inhibits downstream of IKK and Bay 11-7082 has been reported to be apparently not specific for NF-κB pathway [22]. Therefore our study provides further evidence for the importance of NF-κB in the survival of LCLs and indicates effectiveness of DHMEQ in the treatment of EBV-infected transformed lymphocytes.

We also showed that DHMEQ inhibits constitutive NF-κB activation in B lymphocytes expressing LMP1, eliminates these cells from PBMC, and inhibits the outgrowth of lymphoblastic cells. The results indicate that B lymphocytes become dependent on NF-κB for proliferation and survival within several days after EBV infection. Although previous data indicate that not only NF-κB but also other signals like mitogen-activated protein kinases are involved in transformation of lymphocytes to LCL cells [19], the results in this study indicates that abrogation of constitutive NF-κB activity appears to be sufficient to prevent transformation of EBV-infected lymphocytes. Previous reports underscored constitutive NF-κB activity as a molecular target in LCL cells [20,21,23]. Our study shows a new insight that constitutive NF-κB activity is a common molecular target in EBV-infected transformed and untransformed lymphocytes.

Recent reports showed that EBV viral load is a useful marker for disease status of lymphoproliferative diseases or lymphomas in patients with immunosuppression [24]. We showed that DHMEQ treatment prevented the increase of EBV viral load in PBMC. The reduction of EBV viral load in PBMC by DHMEQ indicates not only that the elimination of lymphocytes infected by EBV contributes to the reduction, but also that the replication of EBV virus may depend on NF-κB activity. However, previous studies showed that NF-κB activity does not promote replication of EBV virus, but rather inhibits its replication [25]. Therefore, reduction of viral load in lymphocytes infected with EBV treated with DHMEQ appears to be due to the elimination of lymphocytes infected with EBV. Collectively, early detection of the increase of EBV viral load and purging infected cells under transformation by a NF-κB inhibitor may contribute to the preventive intervention against lymphoproliferative diseases in patients with profound immunosuppression.

Our results suggest that the effects of DHMEQ depend on the down-regulation of NF-κB-dependent genes that control apoptosis. Down-regulation of c-FLIP, involved in anti-apoptosis blocking caspase-8, as well as Bfl-1, Bcl-XL and c-IAP, involved in the anti-apoptosis blocking caspase-9, by DHMEQ may result in activation of membranous and mitochondrial pathways, respectively [26]. This implies the possibility that in EBV-infected lymphocytes, the induction of anti-apoptotic genes is counteracting the apoptotic pressure and preventing these cells from undergoing apoptosis.

The mice treated with DHMEQ in 1% DMSO did not show any relevant signs of toxicity such as body weight loss in this experiment. The dose of DHMEQ administered in this experiment was 12 mg/kg three times a week, far less than the LD_{50} of DHMEQ, 180 mg/kg (Naoki Matsumoto, K.U., unpublished observation, July 1999). Results of our in vivo model suggest that DHMEQ may be feasible and less toxic at an effective dose, although the pharmacokinetics has not yet been elucidated. In our NOG mice model, the results indicate that local administration of DHMEQ can prevent primary tumor growth without significant signs of toxicity. Additional experiments, which include intraperitoneal and intravenous administration of DHMEQ, will further confirm efficacy of DHMEQ against LCLs *in vivo*.

Our recent study also indicates that DHMEQ has little effect on the viability of PBMC or purified B cells *in vitro* under almost the same experimental condition as this study [27]. These *in vitro* and *in vivo* results suggest a favorable toxic profile and potent NF-κB inhibitory effect by DHMEQ. Thus, DHMEQ appears to be a candidate for the treatment of EBV-associated lymphoproliferative diseases as well as for their chemoprevention.

In conclusion, our study indicates that the unique NF-κB inhibitor DHMEQ is a potential compound that targets constitutive activation of NF-κB in EBV-infected transformed and untransformed B cells. Because EBV-associated lymphoproliferative diseases are life-threatening and the prognosis of AIDS-associated lymphomas is extremely unfavorable, our results support preventive intervention with a NF-κB inhibitor as a new strategy in patients with immunosuppression.

Acknowledgments

This work was supported in part by Grants-in-Aid for Scientific Research from the Japan Society for Promotion of Science (R.H. and T.W.). This work was also supported by grants from the Japanese Ministries of Education, Culture, Sport Science and Technology and Health, Labour and Welfare, as well as the Human Health Science of Japan (N.Y.).

References

[1] J.I. Cohen, Epstein–Barr virus infection, N. Engl. J. Med 343 (2000) 481–492.
[2] K.F. Macsween, D.H. Crawford, Epstein–Barr virus-recent advances, Lancet Infect. Dis 3 (2003) 131–140.
[3] E. Klein, L.L. Kis, G. Klein, Epstein–Barr virus infection in humans: from harmless to life endangering virus-lymphocyte interactions, Oncogene 26 (2007) 1297–1305.

[4] S. Gottschalk, C.M. Rooney, H.E. Heslop, Post-transplant lymphoproliferative disorders, Annu. Rev. Med 56 (2005) 29–44.
[5] C. Diamond, T.H. Taylor, T. Aboumrad, H. Anton-Culver, Changes in acquired immunodeficiency syndrome-related non-Hodgkin lymphoma in the era of highly active antiretroviral therapy: incidence, presentation, treatment, and survival, Cancer 106 (2006) 128–135.
[6] Y. Hoshida, J.X. Xu, S. Fujita, I. Nakamichi, J. Ikeda, Y. Tomita, S. Nakatsuka, J. Tamaru, A. Iizuka, T. Takeuchi, K. Aozasa, Lymphoproliferative disorders in rheumatoid arthritis: clinicopathological analysis of 76 cases in relation to methotrexate medication, J. Rheumatol 34 (2007) 322–331.
[7] D.C. Guttridge, C. Albanese, J.Y. Reuther, R.G. Pestell, A.S. Baldwin Jr., NF-kappaB controls cell growth and differentiation through transcriptional regulation of cyclin D1, Mol. Cell. Biol. 19 (1999) 5785–5799.
[8] O. Devergne, E. Hatzivassiliou, K.M. Izumi, K.M. Kaye, M.F. Kleijnen, E. Kieff, G. Mosialos, Association of TRAF1, TRAF2, and TRAF3 with an Epstein–Barr virus LMP1 domain important for B-lymphocyte transformation: role in NF-kappaB activation, Mol. Cell. Biol. 16 (1996) 7098–7108.
[9] T.D. Gilmore, Introduction to NF-kappaB: players, pathways, perspectives, Oncogene 25 (2006) 6680–6684.
[10] N. Matsumoto, A. Ariga, S. To-e, H. Nakamura, N. Agata, S. Hirano, J. Inoue, K. Umezawa, Synthesis of NF-kappaB activation inhibitors derived from epoxyquinomicin C, Bioorg. Med. Chem. Lett. 10 (2000) 865–869.
[11] A. Ariga, J. Namekawa, N. Matsumoto, J. Inoue, K. Umezawa, Inhibition of tumor necrosis factor-alpha-induced nuclear translocation and activation of NF-kappa B by dehydroxymethylepoxyquinomicin, J. Biol. Chem. 277 (2002) 24625–24630.
[12] G. Miller, M. Lipman, Comparison of the yield of infectious virus from clones of human and simian lymphoblastoid lines transformed by Epstein–Barr virus, J. Exp. Med 138 (1973) 1398–1412.
[13] N.C. Andrews, D.V. Faller, A rapid micropreparation technique for extraction of DNA-binding proteins from limiting numbers of mammalian cells, Nucleic Acids Res. 19 (1991) 2499.
[14] J. Inoue, L.D. Kerr, L.J. Ransone, E. Bengal, T. Hunter, I.M. Verma, c-rel activates but v-rel suppresses transcription from kappa B sites, Proc. Natl. Acad. Sci. USA 88 (1991) 3715–3719.
[15] M.Z. Dewan, J.N. Uchihara, K. Terashima, M. Honda, T. Sata, M. Ito, N. Fujii, K. Uozumi, K. Tsukasaki, M. Tomonaga, Y. Kubuki, A. Okayama, M. Toi, N. Mori, N. Yamamoto, Efficient intervention of growth and infiltration of primary adult T-cell leukemia cells by an HIV protease inhibitor, ritonavir, Blood 107 (2006) 716–724.
[16] M. Watanabe, M.Z. Dewan, T. Okamura, M. Sasaki, K. Itoh, M. Higashihara, H. Mizoguchi, M. Honda, T. Sata, T. Watanabe, N. Yamamoto, K. Umezawa, R. Horie, A novel NF-kappaB inhibitor DHMEQ selectively targets constitutive NF-kappaB activity and induces apoptosis of multiple myeloma cells in vitro and in vivo, Int. J. Cancer 114 (2005) 32–38.
[17] H. Kimura, M. Morita, Y. Yabuta, K. Kuzushima, K. Kato, S. Kojima, T. Matsuyama, T. Morishima, Quantitative analysis of Epstein–Barr virus load by using a real-time PCR assay, J. Clin. Microbiol. 37 (1999) 132–136.
[18] J. Dutta, Y. Fan, N. Gupta, G. Fan, C. Gelinas, Current insights into the regulation of programmed cell death by NF-kappaB, Oncogene 25 (2006) 6800–6816.
[19] E.D. Cahir McFarland, K.M. Izumi, G. Mosialos, Epstein–Barr virus transformation: involvement of latent membrane protein 1-mediated activation of NF-kappaB, Oncogene 18 (1999) 6959–6964.
[20] E.D. Cahir-McFarland, K. Carter, A. Rosenwald, J.M. Giltnane, S.E. Henrickson, L.M. Staudt, E. Kieff, Role of NF-kappa B in cell survival and transcription of latent membrane protein 1-expressing or Epstein–Barr virus latency III-infected cells, J. Virol 78 (2004) 4108–4119.
[21] S.A. Keller, D. Hernandez-Hopkins, J. Vider, V. Ponomarev, E. Hyjek, E.J. Schattner, E. Cesarman, NF-kappaB is essential for the progression of KSHV- and EBV-infected lymphomas in vivo, Blood 107 (2006) 3295–3302.
[22] J.W. Pierce, R. Schoenleber, G. Jesmok, J. Best, S.A. Moore, T. Collins, M.E. Gerritsen, Novel inhibitors of cytokine-induced IkappaBalpha phosphorylation and endothelial cell adhesion molecule expression show anti-inflammatory effects in vivo, J. Biol. Chem. 272 (1997) 21096–21103.
[23] E.D. Cahir-McFarland, D.M. Davidson, S.L. Schauer, J. Duong, E. Kieff, NF-kappa B inhibition causes spontaneous apoptosis in Epstein–Barr virus-transformed lymphoblastoid cells, Proc. Natl. Acad. Sci. USA 97 (2000) 6055–6060.
[24] S.M. Aalto, E. Juvonen, J. Tarkkanen, L. Volin, T. Ruutu, P.S. Mattila, H. Piiparinen, S. Knuutila, K. Hedman, Lymphoproliferative disease after allogeneic stem cell transplantation–pre-emptive diagnosis by quantification of Epstein–Barr virus DNA in serum, J. Clin. Virol 28 (2003) 275–283.
[25] H.J. Brown, M.J. Song, H. Deng, T.T. Wu, G. Cheng, R. Sun, NF-kappaB inhibits gammaherpesvirus lytic replication, J. Virol 77 (2003) 8532–8540.
[26] J.M. Adams, Ways of dying: multiple pathways to apoptosis, In: Genes Dev, 17 (2003) 2481–2495.
[27] R. Horie, M. Watanabe, T. Okamura, M. Taira, M. Shoda, T. Motoji, A. Utsunomiya, T. Watanabe, M. Higashihara, K. Umezawa, DHMEQ, a new NF-kappaB inhibitor, induces apoptosis and enhances fludarabine effects on chronic lymphocytic leukemia cells, Leukemia 20 (2006) 800–806.

Biochemical and Biophysical Research Communications 376 (2008) 310–314

Contents lists available at ScienceDirect

Biochemical and Biophysical Research Communications

journal homepage: www.elsevier.com/locate/ybbrc

Identification of the RelA domain responsible for action of a new NF-κB inhibitor DHMEQ

Mariko Watanabe [a,1], Makoto Nakashima [a,1], Tomiteru Togano [a], Masaaki Higashihara [a], Toshiki Watanabe [b], Kazuo Umezawa [c], Ryouichi Horie [a,*]

[a] Department of Hematology, School of Medicine, Kitasato University, 1-15-1 Kitasato, Sagamihara, Kanagawa 228-8555, Japan
[b] Laboratory of Tumor Cell Biology, Department of Medical Genome Sciences, Graduate School of Frontier Sciences, University of Tokyo, 4-6-1 Shirokanedai, Minato-ku, Tokyo 108-8639, Japan
[c] Department of Applied Chemistry, Faculty of Science and Technology, Keio University, 3-14-1 Hiyoshi, Kohoku-ku, Yokohama, Kanagawa 223-0061, Japan

ARTICLE INFO

Article history:
Received 24 August 2008
Available online 7 September 2008

Keywords:
NF-κB inhibitor
DHMEQ
RelA
p50

ABSTRACT

A new NF-κB inhibitor dehydroxymethylepoxyquinomicin (DHMEQ) has a potential to be applied to clinical medicine as an anti-cancer and anti-inflammatory agent. DHMEQ inhibits localization of NF-κB in the nucleus and the inhibitory effect by DHMEQ is more potent on p50/RelA than on p50 homodimer. However, a molecular target of DHMEQ is unknown. In this study, we identified residues CEGRSAGSI, which appear in RelA (amino acids 38–46), c-Rel (28–36), and RelB (144–152), but not in p50 and p52, as a target of DHMEQ. As a possible mechanism, we propose that DHMEQ accesses CEGRSAGSI domain recognizing RSAGSI structure and directly binds to cysteine. This target domain appears to be unique among mammalian proteins. The results obtained in this study may provide better understanding of the action of DHMEQ and a key for developing a new NF-κB inhibitor with more potent activity.

Dehydroxymethylepoxyquinomicin (DHMEQ) is a new NF-κB inhibitor that is a 5-dehydroxymethyl derivative of the novel compound epoxyquinomicin C with a 4-hydroxy-5,6-epoxycyclohexenone structure like panepoxydone [1]. NF-κB represents a family of inducible transcription factors and activation of NF-κB has been connected with resistance against apoptosis and tumorigenesis [2,3]. Accumulating evidences indicate that DHMEQ is a promising compound to be applied to clinical medicine as an anti-cancer and anti-inflammatory agent [4].

We have shown that DHMEQ acts at the downstream of IκB kinase and inhibits localization of NF-κB in the nucleus. DHMEQ did not inhibit nuclear localization of SV-40 large T antigen or Smad2, suggesting that DHMEQ does not target the general mechanism involved in nuclear localization, but targets some other mechanism that is more specific to the NF-κB pathway [5]. Furthermore, our previous studies showed that DHMEQ inhibits constitutive NF-κB activity consisting of p50/RelA (p65), but its effect is less potent against p50 homodimer [6,7]. This specific action of DHMEQ may explain why DHMEQ can effectively induce apoptosis in cancer cells with constitutive NF-κB activity consisting of p50/RelA, but does not affect normal resting lymphocytes, whose NF-κB activity consists mainly of p50 homodimer without RelA. However, the molecular target of DHMEQ and the reason, which explains difference in the specificity of DHMEQ between p50/RelA and p50 homodimer are entirely unknown.

In this study, we identified a molecular target of DHMEQ and elucidated the reason for the difference in the specificity of DHMEQ between p50/RelA and p50 homodimer by comparing the RelA domain with the corresponding domain in p50 as well as other NF-κB family proteins.

Materials and methods

Cell cultures. HeLa cell line was obtained from the Japanese Cancer Research Resources Bank (Tokyo, Japan). KMH2 cell line was purchased from the German Collection of Microorganisms and Cell Cultures (Braunschweig, Germany). The TL-Om1 cell line was a gift from Dr. K. Sugamura, Tohoku University. Non-adherent cell lines were cultured in RPMI 1640 medium and adherent cells were cultured in Dulbecco's modified Eagle's medium (DMEM) with supplementation of recommended concentrations of fetal bovine serum (FBS) and antibiotics.

Chemicals. We used (−)-DHMEQ, which is 10 times more potent than (+)-DHMEQ. (−)-DHMEQ was synthesized as previously described [1]. DHMEQ was dissolved in dimethyl sulfoxide (DMSO) for use in experiments. Human TNF-α was purchased from PEPRO TECH, INC. (Rocky Hill, NJ, USA). Dithiothreitol (DTT) and isopropyl

* Corresponding author. Fax: +81 42 778 8441.
E-mail address: rhorie@med.kitasato-u.ac.jp (R. Horie).
[1] These authors equally contributed to this work.

0006-291X/$ - see front matter © 2008 Elsevier Inc. All rights reserved.
doi:10.1016/j.bbrc.2008.08.148

1-thio-β-D-galactoside (IPTG) were purchased from Promega (Madison, WI, USA).

Plasmids and mutagenesis. Wild-type human RelA cDNA was cloned by polymerase chain reaction (PCR) using cDNA from TL-Om1 cells and was then inserted into pEGFP-N1 expression vector (Clontech, Mountain View, CA, USA). N-terminal deletion mutants of RelA were prepared by PCR using wild-type RelA cDNA and were then cloned into pEGFP-C1 expression vector (Clontech). Wild-type human cDNAs for p50, p52, and c-Rel were cloned by PCR using cDNA from KMH2 cells and inserted into pGFPN-1 expression vector (Clontech). The expression vectors for IκBα and RelB cDNA were generous gifts from Dr. J. Inoue at Tokyo University. Amino acid numbers corresponding to the region cloned into the expression vectors and the National Center for Biotechnology Information (NCBI) accession numbers. of each corresponding protein are as follows: RelA (amino acids 1–551, NCBI Accession No. NM_021975), c-Rel (amino acids 1–619, NCBI Accession No. NM_002908), p50 (amino acids 1–436, NCBI Accession No. NM_003998) and p52 (amino acids 1–405, NCBI Accession No. NM_001077494).

Using the method for mutagenesis by Kunkel et al., we obtained the expression vectors that express mutant protein: RelAmut [RelA RSAGSI (amino acids 41–46) was replaced by the corresponding domain of p50 PSHGGL (amino acids 65–70)], RelAC38S (amino acid 38 cysteine of RelA was replaced by serine), and p50mut (p50 PSHGGL was replaced by corresponding domain of RelA RSAGSI) [8].

Immunofluorescence. To observe the localization of NF-κB family proteins, 1×10^5 of HeLa cells were transfected with 1 μg of Green Fluorescent Protein (GFP) fused vector plasmid and 1 μg of IκBα expression vector using Lipofectamine 2000 reagent (Invitrogen, Carlsbad, CA, USA) according to the manufacturer's instructions. HeLa cells seeded onto poly-L-lysine-coated culture coverglass (MATSUNAMI, Osaka, Japan) served for transfection. After an additional 18 h of culturing, cells were pretreated with or without 10 μg/ml of DHMEQ for 1 h before stimulation with or without 20 ng/ml of TNF-α for 15 min. Subsequently, cells were washed in phosphate-buffered saline (PBS) three times, fixed in 4% paraformaldehyde phosphate buffer solution (Wako, Osaka, Japan) for 10 min and washed in PBS three times. After final washing, the coverslips were dried and mounted on slides with a Perma Fluoro anti-fade reagent (Therme Shandon Co., Pittsburgh, PA, USA). Fluorescence signals were detected using confocal microscopy (Radiance 2000, Bio-Rad Laboratories, Hercules, CA, USA).

Immunohistochemistry. Cells were immunostained with antibodies and fluorescence signals were detected using confocal microscopy. Cytospin samples were prepared using 1×10^5 cells and were first washed three times with PBS. Cells were then fixed with methanol or 10% paraformaldehyde for 10 min at room temperature and washed three times in PBS. Samples were incubated with primary antibody at the concentration of 5 μg/ml at 4 °C overnight and washed with PBS three times. After incubation with fluorescence-labeled secondary antibody for 30 min at 37 °C, samples were washed three times in PBS and covered with a Perma Fluoro anti-fade reagent (Therme Shandon Co.). Fluorescence signals were detected using confocal microscopy (Radiance 2000) (Bio-Rad Laboratories). Antibodies used were as follows: anti-NF-κB p65 SUBUNIT mouse monoclonal antibody (Chemicon International, Temecula, CA, USA) and goat anti-mouse IgG FITC conjugated antibody (Santa Cruz Biotechnology, Inc.).

Production of glutathione S-transferase (GST) fusion protein. Human RelA cDNA corresponding to amino acids 1–327 was amplified by PCR using wild-type RelA expression vector as a template and then cloned into pGEX-5X-1 vector (GE Healthcare). We created expression vectors for amino acids 1–327 of RelAC38S using the same strategy. Recombinant proteins were expressed in *Escherichia coli DH5α* (Takara Kyoto, Japan) as GST fusion proteins at 30 °C for 4 h under induction with 0.1 mM IPTG. Glutathione *S*-transferase and GST fusion proteins were prepared by standard methods [9].

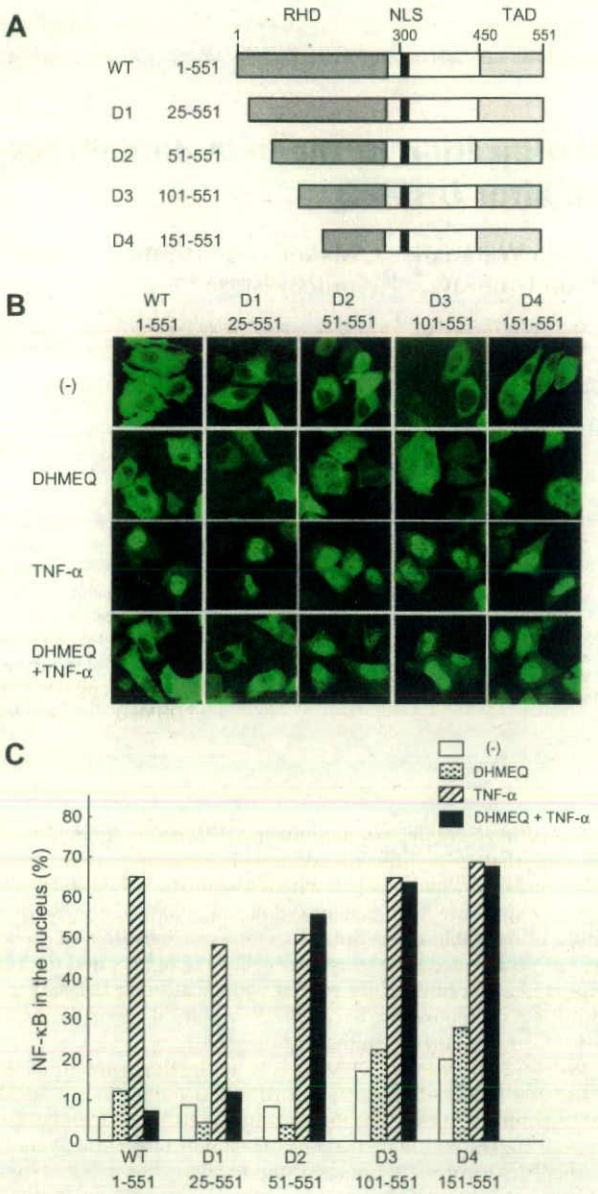

Fig. 1. The N-terminus of RelA (amino acids 25–50) is responsible for the inhibition of the nuclear localization of RelA by DHMEQ. (A) Primary domain structure of wild-type and its truncation constructs of RelA. The location of Rel homology domain (RHD), nuclear localization signal (NLS), and trans activation domain (TAD) are presented according to the previous study [18]. The numbers on the left and those on the top indicate the amino acid numbers of RelA. (B) Fluorescence analysis to determine the RelA domain responsible for the inhibition of the TNF-α-mediated localization of RelA in the nucleus by DHMEQ. HeLa cells were transfected with the indicated cDNA expression vectors for GFP fusion constructs and the expression vector for IκBα. After 18 h, cells were stimulated with or without 20 ng/ml of TNF-α for 15 min under pretreatment with or without 10 μg/ml of DHMEQ for 1 h as indicated on the left. Location of the constructs visualized by autofluorescence of GFP was observed by confocal laser microscopy. Representative distribution patterns that characterize each group are presented as representative figures. The RelA constructs used are indicated on the top. (C) Quantitative analysis. For quantification, 300 cells were scored for fluorescence location in the nucleus. The data are representative of triplicate experiments.

The recombinant proteins were immobilized onto GST-binding resin (Novagen, Madison, WI, USA) and served for the experiments after washing with PBS five times.

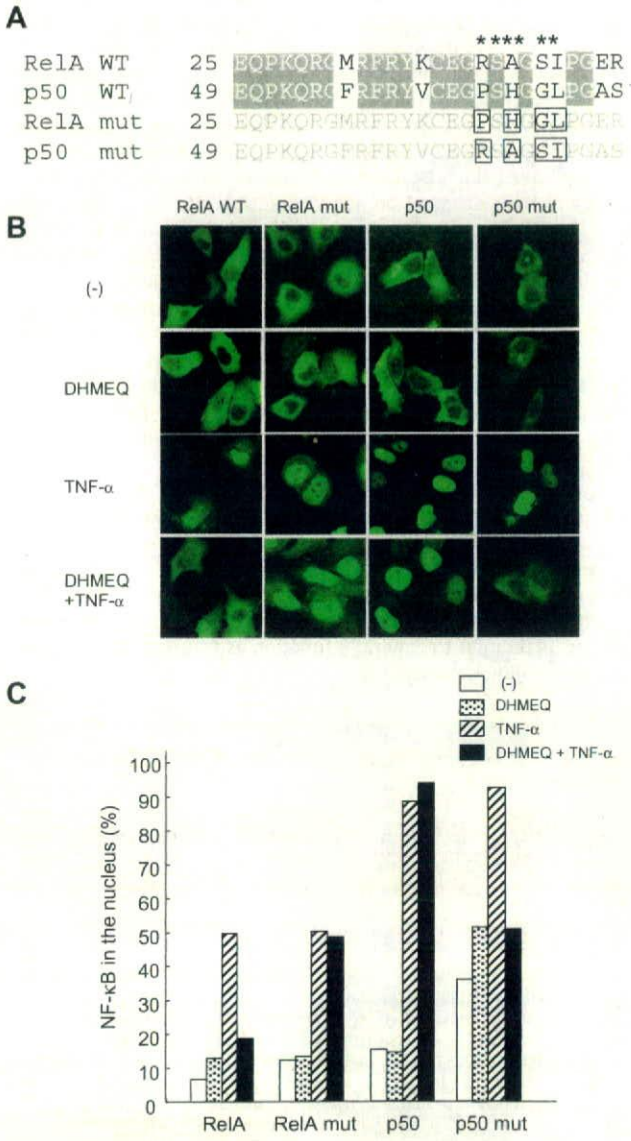

Fig. 2. The domain RSAGSI (amino acids 41–46) of RelA is responsible for the DHMEQ-mediated inhibition of the nuclear localization of RelA and the differentiation of the effect of DHMEQ on p50. (A) Comparison of the amino acid alignment of RelA, p50, and their mutants. RelA RSAGSI (amino acids 41–46) and p50 PSHGGL (amino acids 65–70), which are indicated by asterisks, are less conserved within the domain corresponding to that of RelA responsible for DHMEQ action (amino acids 25–50). Conserved residues between RelA and p50 are indicated on a gray background. The structures of RelAmut and p50mut are described in the Materials and methods section. Amino acid residues replaced are indicated by open squares. The numbers on the left indicate the amino acid number of each protein. (B) Fluorescence analysis to determine the domain that differentiates the action of DHMEQ on RelA and p50. HeLa cells were transfected with the indicated cDNA expression vectors for GFP fusion constructs and the expression vector for IκBα, treated, and observed as described in the legend for Fig. 1B. Constructs used are indicated on the top. (C) Quantitative analysis. Quantification was done as described in the legend for Fig. 1C. The data are representative of triplicate experiments.

Results and discussion

Identification of the RelA domain responsible for DHMEQ-mediated inhibition of nuclear localization of RelA

Previous observation indicated that DHMEQ does not target the general mechanism involved in nuclear transportation, but targets some other mechanism that is more specific to NF-κB [5]. Therefore, we first examined the effect of DHMEQ on RelA deletion mutants, which lack an N-terminus and contain residues spanning 25–551 (D1), 51–551 (D2), 101–551 (D3), and 151–551 (D4) of RelA (Fig. 1A). These RelA mutants and wild-type RelA were constructed as GFP fusion proteins and transfected into HeLa cells. Expression of wild-type RelA in HeLa cells was characterized by

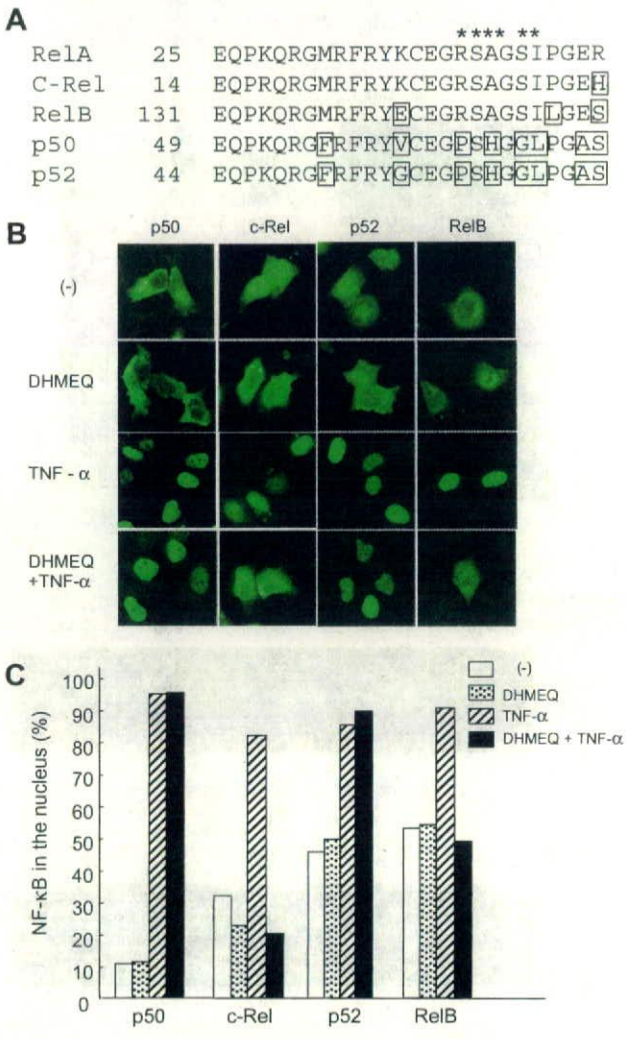

Fig. 3. DHMEQ inhibits the localization of c-Rel and RelB, which retain RelA RSAGSI, but not that of p52, which has p50 PSHGGL. (A) Comparison of the amino acid alignment of RelA, c-Rel, RelB, p50, and p52. Amino acid alignment corresponding to RelA RSAGSI (amino acids 41–46) is indicated by asterisks. Residues not conserved, when compared with RelA, are indicated by open squares. The numbers on the left indicate the amino acid number of each protein. (B) Fluorescence analysis to differentiate the response for the action of DHMEQ on NF-κB family proteins. HeLa cells were transfected with the indicated cDNA expression vectors for GFP fusion constructs and the expression vector for IκBα, treated, and observed as described in the legend for Fig. 1B. Constructs used are indicated on the top. (C) Quantitative analysis. Quantification was done as described in the legend for Fig. 1C. The data are representative of triplicate experiments.

predominant cytoplasmic distribution, as previously reported [5]. We cotransfected RelA constructs and IκBα, because transfection of RelA D4 alone caused nuclear localization (data not shown), which might be explained by the loss of IκBα induction ability, as previously reported [10]. Under this experimental condition, transfection of wild-type and each deletion mutant was characterized by predominant cytoplasmic distribution (Fig. 1B, top panel). Treatment with DHMEQ did not affect this distribution pattern (Fig. 1B, second panel). TNF-α stimulation changed their distribution from a cytoplasmic to a nuclear pattern (Fig. 1B, third panel). Pretreatment with DHMEQ inhibited the TNF-α-mediated nuclear localization when wild-type and D1 constructs were used, whereas DHMEQ did not inhibit nuclear localization when D2, D3, and D4 constructs were used (Fig. 1B, bottom panels; Fig. 1C). These observations indicate that the RelA domain, which is responsible for DHMEQ-mediated inhibition of nuclear localization of NF-κB, resides within residues 25–50 of RelA.

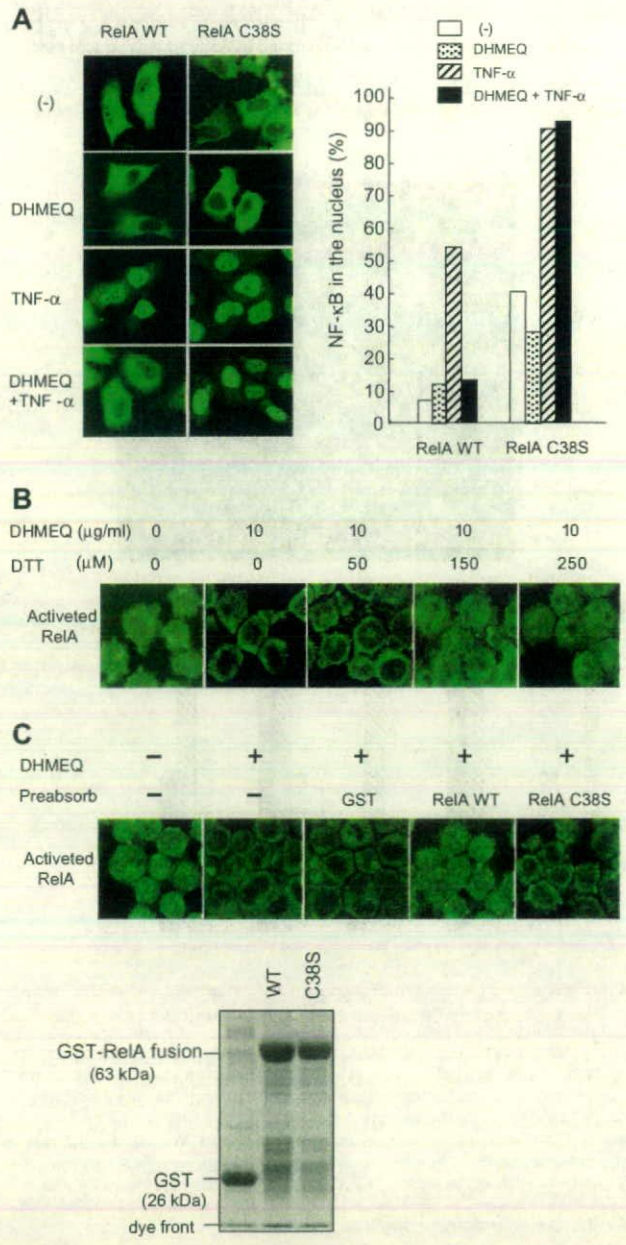

The RelA domain RSAGSI differentiates the effect by DHMEQ on RelA and p50

Our previous observation showed that DHMEQ inhibits constitutive NF-κB activity consisting of p50/RelA, but its effect is less potent against p50 homodimer [6,7]. To identify the amino acid residues, which are responsible for the different effect by DHMEQ on RelA and p50, we analyzed the amino acid homology between RelA and p50 and took notice of the domain RSAGSI spanning residues 41–46 of RelA (Fig. 2A). Transfection of GFP-fused p50 alone in Hela cells caused nuclear localization (data not shown). A previous report showed that IκBα associates not only with RelA, but also with p50 [11]. Therefore, we cotransfected expression plasmids for GFP-fused RelA, p50 or their mutants with that for IκBα, which enabled us to observe the TNF-α-dependent change in their distribution. Replacement of RSAGSI (amino acids 41–46) of RelA with the corresponding domain of p50 PSHGGL (amino acids 65–70), which is indicated as RelAmut, abolished the effect of DHMEQ (Fig. 2B, second row from the left; Fig. 2C). Inversely, replacement of p50 PSHGGL with the corresponding domain of RelA (RSAGSI), which is indicated as p50mut, recovered the effect of DHMEQ (Fig. 2B, third and fourth rows from the left; Fig. 2C). These observations indicate that the domain RSAGSI spanning residues 41–46 of RelA is responsible for the DHMEQ-mediated inhibition of nuclear localization of RelA and the differentiation of the effect of DHMEQ on p50.

The result indicates that inhibitory effect of DHMEQ operates if at least one partner of dimeric NF-κB complex is RelA. This selective action of DHMEQ appears to be important for its specificity to exert anti-cancer and anti-inflammatory activity, because p50/RelA plays a major role in cancer cell growth and inflammatory activity, whereas p50 homodimer, which lacks transactivation activity, is thought to generally function as transcriptional repressors for p50/RelA activity [12].

DHMEQ inhibits TNF-mediated localization of c-Rel and RelB, which retain RelA RSAGSI, but not that of p52 having p50 PSHGGL in the nucleus

RelA RSAGSI is shared among RelA, c-Rel, and RelB, whereas p50 PSHGGL is shared between p50 and p52 (Fig. 3A). We next examined the effect of DHMEQ on c-Rel, RelB, and p52. As was the case

Fig. 4. DHMEQ directly targets cysteine 38 of RelA. (A) Fluorescence analysis to observe the effect of replacing cysteine 38 of RelA with serine (left). HeLa cells were transfected with the indicated cDNA expression vectors for GFP fusion constructs, treated, and observed as described in the legend for Fig. 1B. Constructs used are indicated on the top. Quantitative analysis (right). For quantification, 300 cells were scored for fluorescence location in the nucleus. The data are representative of triplicate experiments. (B) Immunofluorescence analysis to determine the effect of DTT on the DHMEQ-mediated inhibition of the translocation of RelA in the nucleus. KMH2 cells with strong and constitutive NF-κB activity were treated with or without 10 μg/ml of DHMEQ for 5 h under pretreatment with DTT for 2 h at culture conditions of 37 °C, 5% CO_2. Cells were subjected to indirect immunofluorescence analysis with antibody for activated RelA, which recognizes RelA NLS, and FITC-conjugated secondary antibody. (C) Nuclear localization of activated RelA was abolished by pre-absorption of DHMEQ with wild-type RelA, but not with RelA C38S, in KMH2 cells with constitutive NF-κB activity (top). Fifty micro molar of DHMEQ and GST or GST-RelA fusion protein attaching to GST-binding resin were co-incubated in phosphate-buffered saline for 1 h at 4 °C. The reaction mixture was centrifuged for 1 min at 5000 rpm at 4 °C and the supernatant was isolated as pre-absorption solution. 1×10^5 KMH2 cells were cultured with or without the pre-absorption solution for 5 h at 37 °C with 5% CO_2. Cells were subjected to indirect immunofluorescence analysis with antibody for activated RelA, which recognizes RelA NLS, and FITC-conjugated secondary antibody. Analysis of GST and GST-RelA fusion proteins (bottom). GST or GST-RelA fusion proteins that were attached to the GST-binding resin used for the co-incubation experiment were boiled after mixture with sample buffer. The samples were separated on a polyacrylamide/10% SDS gel and visualized by Comassie brilliant blue G-250 staining.

with p50, almost all of the cells transfected with c-Rel, RelB, or p52 showed a nuclear localization pattern (data not shown). A previous report showed that IκBα associates not only with RelA and p50, but also with c-Rel on the C-terminal side of Rel homology domain (RHD), indicating the possibility that IκBα also associates with p52 and RelB [11]. Therefore, we cotransfected expression plasmids for GFP-fused c-Rel, RelB, or p52 with that for IκBα, which enabled us to observe the TNF-α-dependent change in their distribution. DHMEQ treatment inhibited TNF-α-dependent nuclear localization in the nucleus of c-Rel and RelB, but not that of p52 (Fig. 3B and C). Above observations are in accordance with the difference between the amino acid alignment of c-Rel and RelB, which retains the RelA RSAGSI domain, and that of p52, which has the p50 PSHGGL domain.

Previous observation indicated that DHMEQ also inhibits the localization of p52/RelB in the nucleus [13]. This inhibition can be explained by the inhibitory effect of DHMEQ on RelB. Because not only p50/RelA but also p52/RelB pathway is reported to involved in survival of cancer cells [3,14], the inhibitory effect of DHMEQ on both NF-κB pathways appears to explain its potent effect.

DHMEQ directly targets cysteine 38 of RelA

Previous reports indicate that sequiterpene lactone (parthenolide) and epoxyquinone A monomer (EpM) exert their NF-κB inhibitory effect through cysteine 38 of RelA [15–17]. This cysteine 38 is located within the domain that we identified to be necessary to exert the action of DHMEQ (RelA amino acids 25–50). Therefore, we examined the effect of substitution of RelA cysteine 38 with serine (RelA C38S) on the DHMEQ-mediated inhibition of localization of RelA in the nucleus. As a result, DHMEQ could not inhibit the TNF-α-mediated localization of RelA C38S in the nucleus, suggesting that DHMEQ appears to target cysteine 38 of RelA (Fig. 4A). To obtain further support for the above notion, we examined the effect of DTT, a potent reducing agent, which protects thiol groups in proteins like cysteine from oxidization, on the effect of DHMEQ. As shown in Fig. 4B, pre-treatment of cells with DTT, which may reduce reactive cysteine residues in the target proteins, inhibited the effect of DHMEQ (Fig. 4B). Importantly, the RelA RSAGSI domain (amino acids 41–46) does not contain cysteine, and cysteine 38 is the only cysteine residue within the RelA domain (amino acids 25–50).

To obtain further evidence that DHMEQ directly targets RelA cysteine 38, we performed a competition assay on the effect of DHMEQ using GST-fused wild-type RelA and RelA C38S. Pre-incubation of DHMEQ with wild-type RelA abrogated DHMEQ-mediated localization of wild-type RelA in the nucleus. However, pre-incubation of DHMEQ with RelA C38S failed to abrogate DHMEQ-mediated localization of wild-type RelA in the nucleus (Fig. 4C). Taken collectively, these results indicate that DHMEQ directly targets cysteine 38 of RelA via thiol group.

A possible mechanism of selective action of DHMEQ among NF-κB family proteins

The residue corresponding to cysteine 38 of RelA is conserved among p50, p52, c-Rel, and RelB; however, DHMEQ inhibits the localization of RelA, c-Rel, and RelB in the nucleus, but not that of p50 and p52. This difference might be due to the structural difference between RSAGSI and PSHGGL; the former is conserved among RelA, c-Rel, and RelB and the latter between p50 and p52. We found that pre-incubation of DHMEQ with a mutant form of RelA, whose RSAGSI domain was replaced with the corresponding domain of p50 (PSHGGL), did not abrogate the effect of DHMEQ (data not shown). Collectively, the simplest explanation of our results might be that DHMEQ targets the CEGRSAGSI domain structure, which appears in RelA, c-Rel, and RelB, directly binding to cysteine by recognizing the RSAGSI structure.

We searched for the existence of alignment RelA CEGRSAGSI (amino acids 38–46) in mammalian proteins using the FASTA version 3.4t26 sequence alignment software package. The result indicated that there was no matching amino acid alignment RelA CEGRSAGSI (amino acids 38–46) in mammalian proteins, further suggesting that the target of DHMEQ is very unique to a subset of NF-κB family proteins.

Acknowledgment

This work was supported by Grants-in Aid from the Ministry of Education, Science, and Culture of Japan to Ryouichi Horie.

References

[1] N. Matsumoto, A. Ariga, S. To-e, H. Nakamura, N. Agata, S. Hirano, J. Inoue, K. Umezawa, Synthesis of NF-κB activation inhibitors derived from epoxyquinomicin C, Bioorg. Med. Chem. Lett. 10 (2000) 865–869.
[2] T.D. Gilmore, Introduction to NF-κB: players, pathways, perspectives, Oncogene 25 (2006) 6680–6684.
[3] D.S. Basseres, A.S. Baldwin, Nuclear factor-κB and inhibitor of κB kinase pathways in oncogenic initiation and progression, Oncogene 25 (2006) 6817–6830.
[4] K. Umezawa, Inhibition of tumor growth by NF-κB inhibitors, Cancer Sci. 97 (2006) 990–995.
[5] A. Ariga, J. Namekawa, N. Matsumoto, J. Inoue, K. Umezawa, Inhibition of tumor necrosis factor-α-induced nuclear translocation and activation of NF-κB by dehydroxymethylepoxyquinomicin, J. Biol. Chem. 277 (2002) 24625–24630.
[6] M. Watanabe, M.Z. Dewan, T. Okamura, M. Sasaki, K. Itoh, M. Higashihara, H. Mizoguchi, M. Honda, T. Sata, T. Watanabe, N. Yamamoto, K. Umezawa, R. Horie, A novel NF-κB inhibitor DHMEQ selectively targets constitutive NF-κB activity and induces apoptosis of multiple myeloma cells in vitro and in vivo, Int. J. Cancer 114 (2005) 32–38.
[7] M. Watanabe, T. Ohsugi, M. Shoda, T. Ishida, S. Aizawa, M. Maruyama-Nagai, A. Utsunomiya, S. Koga, Y. Yamada, S. Kamihira, A. Okayama, H. Kikuchi, K. Uozumi, K. Yamaguchi, M. Higashihara, K. Umezawa, T. Watanabe, R. Horie, Dual targeting of transformed and untransformed HTLV-1-infected T cells by DHMEQ, a potent and selective inhibitor of NF-κB, as a strategy for chemoprevention and therapy of adult T-cell leukemia, Blood 106 (2005) 2462–2471.
[8] T.A. Kunkel, K. Bebenek, J. McClary, Efficient site-directed mutagenesis using uracil-containing DNA, Methods Enzymol. 204 (1991) 125–139.
[9] D.B. Smith, K.S. Johnson, Single-step purification of polypeptides expressed in *Escherichia coli* as fusions with glutathione S-transferase, Gene 67 (1988) 31–40.
[10] A. Hoffmann, G. Natoli, G. Ghosh, Transcriptional regulation via the NF-κB signaling module, Oncogene 25 (2006) 6706–6716.
[11] M. Latimer, M.K. Ernst, L.L. Dunn, M. Drutskaya, N.R. Rice, The N-terminal domain of IκBα masks the nuclear localization signal(s) of p50 and c-Rel homodimers, Mol. Cell. Biol. 18 (1998) 2640–2649.
[12] H. Guan, S. Hou, R.P. Ricciardi, DNA binding of repressor nuclear factor-κB p50/p50 depends on phosphorylation of Ser337 by the protein kinase A catalytic subunit, J. Biol. Chem. 280 (2005) 9957–9962.
[13] G. Matsumoto, J. Namekawa, M. Muta, T. Nakamura, H. Bando, K. Tohyama, M. Toi, K. Umezawa, Targeting of nuclear factor κB Pathways by dehydroxymethylepoxyquinomicin, a novel inhibitor of breast carcinomas: antitumor and antiangiogenic potential in vivo, Clin. Cancer Res. 11 (2005) 1287–1293.
[14] E. Dejardin, The alternative NF-κB pathway from biochemistry to biology: pitfalls and promises for future drug development, Biochem. Pharmacol. 72 (2006) 1161–1179.
[15] A.J. Garcia-Pineres, V. Castro, G. Mora, T.J. Schmidt, E. Strunck, H.L. Pahl, I. Merfort, Cysteine 38 in p65/NF-κB plays a crucial role in DNA binding inhibition by sesquiterpene lactones, J. Biol. Chem. 276 (2001) 39713–39720.
[16] A.J. Garcia-Pineres, M.T. Lindenmeyer, I. Merfort, Role of cysteine residues of p65/NF-κB on the inhibition by the sesquiterpene lactone parthenolide and *N*-ethyl maleimide, and on its transactivating potential, Life Sci. 75 (2004) 841–856.
[17] M.C. Liang, S. Bardhan, J.A. Porco Jr., T.D. Gilmore, The synthetic epoxyquinoids jesterone dimer and epoxyquinone A monomer induce apoptosis and inhibit REL (human c-Rel) DNA binding in an IκBα-deficient diffuse large B-cell lymphoma cell line, Cancer Lett. 241 (2006) 69–78.
[18] E.W. Harhaj, S.C. Sun, Regulation of RelA subcellular localization by a putative nuclear export signal and p50, Mol. Cell. Biol. 19 (1999) 7088–7095.

Impaired Tax-specific T-cell responses with insufficient control of HTLV-1 in a subgroup of individuals at asymptomatic and smoldering stages

Yukiko Shimizu,[1] Ayako Takamori,[1] Atae Utsunomiya,[2] Mayumi Kurimura,[3] Yoshihisa Yamano,[4] Masakatsu Hishizawa,[5] Atsuhiko Hasegawa,[1] Fumiaki Kondo,[1] Kiyoshi Kurihara,[1] Nanae Harashima,[1] Toshiki Watanabe,[6] Jun Okamura,[7] Takao Masuda[1] and Mari Kannagi[1,8]

[1]Department of Immunotherapeutics, Tokyo Medical and Dental University, Graduate School, 1-5-45 Yushima, Bunkyo-ku, Tokyo 113-8519; [2]Department of Hematology, Imamura Bun-in Hospital, 11-23 Kamoike-Shinmachi, Kagoshima 890-0064; [3]Kamigotoh Hospital, Shin-Kamigoto-cho, Minami-Matsuura-gun, Nagasaki 857-4404; [4]Department of Genome Science, Institute of Medical Science, St. Marianna University School of Medicine, Miyamae-Ku, Kawasaki, Kanagawa 216-8512; [5]Department of Hematology and Oncology, Graduate School of Medicine, Kyoto University, Sakyo-ku, Kyoto 505-8507; [6]Laboratory of Tumor Cell Biology, Department of Medical Genome Science, Graduate School of Frontier Sciences, University of Tokyo, Minato-ku, Tokyo 108-8639; [7]Clinical Research Division, National Kyusyu Cancer Center, Minami-ku, Fukuoka 811-1395, Japan

(Received August 14, 2008/Revised November 4, 2008/Accepted November 9, 2008/Online publication December 18, 2008)

Human T-cell leukemia virus type-1 (HTLV-1)-specific T-cell immunity, a potential antitumor surveillance system *in vivo*, is impaired in adult T-cell leukemia (ATL). In this study, we aimed to clarify whether the T-cell insufficiency in ATL is present before the disease onset or occurs as a consequence of the disease. We investigated T-cell responses against Tax protein in peripheral blood mononuclear cells (PBMCs) from individuals at earlier stages of HTLV-1-infection, including 21 asymptomatic HTLV-1 carriers (ACs) and four patients with smoldering-type ATL (sATL), whose peripheral lymphocyte count was in normal range. About 30% of samples tested showed clear Tax-specific interferon (IFN)-γ producing responses. Proviral loads in this group were significantly lower than those in the other less-specific response group. The latter group was further divided to two subgroups with or without emergence of Tax-specific responses following depletion of CC chemokine receptor 4 (CCR4)$^+$ cells that contained HTLV-1-infected cells. In the PBMCs with Tax-specific responses, CD8$^+$ cells efficiently suppressed HTLV-1 p19 production in culture. The remaining group without the emergence of Tax-specific response after CCR4$^+$ cell-depletion included at least two sATL and one AC samples, which spontaneously produced HTLV-1 p19 in culture, where tetramer-binding, Tax-specific cytotoxic T-lymphocytes were either undetectable or unresponsive. Our results indicated that HTLV-1-specific T-cell responsiveness widely differed among HTLV-1 carriers, and that impairment of HTLV-1-specific T-cell responses was observed not only in advanced ATL patients but also in a subpopulation at earlier stages, which was associated with insufficient control of HTLV-1. (*Cancer Sci* 2009; 100: 481–489)

Human T-cell leukemia virus type 1 (HTLV-1) is the etiological agent of adult T-cell leukemia (ATL).[1,2] Although the majority of HTLV-1-infected individuals remain asymptomatic throughout their lives, about 5% develop ATL during or after middle age and another small population develops HTLV-1-associated myelopathy/tropical spastic paraparesis (HAM/TSP) and a variety of chronic inflammatory diseases.[3–7] Several epidemiological risk factors have been suggested to be associated with ATL development, including vertical transmission, gender (greater incidence in males than in females),[4,8] and increased numbers of abnormal lymphocytes associated with elevated HTLV-1 proviral loads.[9,10] However, elevation in HTLV-1 proviral loads is also a feature of HAM/TSP patients.[7,11]

ATL is known to be an immunosuppressive condition.[3] Recent reports have shown that ATL cells frequently express Foxp3 and the chemokine receptor CCR4, in addition to CD4 and CD25.[12–16] These molecules are also expressed in regulatory T-cells (Tregs).[17–20] Although isolated ATL cells do not always exhibit suppressive functions *in vitro*, the common phenotypes shared by ATL cells and Tregs suggest that ATL cells may share a common origin with Tregs, or possess immunoregulatory properties.[21] General immunosuppression may be present not only in ATL patients, but also in asymptomatic HTLV-1 carriers (ACs) to some extent.[22,23]

There is a clear difference between ATL and HAM/TSP patients in the host T-cell responses against HTLV-1. Outgrowth of CD8$^+$ HTLV-1-specific cytotoxic T-lymphocytes (CTLs) in response to *in vitro* stimulation is frequently found in peripheral blood mononuclear cell (PBMC) cultures from HAM/TSP patients, but rarely observed in those from ATL patients.[24–26] These CTLs have anti-HTLV-1 effects, as elimination of CD8$^+$ cells among PBMCs from HAM/TSP patients induces HTLV-1 expression during subsequent cell culture.[27,28] HTLV-1 Tax-specific CTL responses are strongly activated in some ATL patients who obtained complete remission after hematopoietic stem cell transplantation (HSCT), but are not observed in the same patients before transplantation.[29] These findings suggest that Tax-specific CTLs may play a role in immunosurveillance for HTLV-1 leukemogenesis.

Studies on a rat model have indicated that the otherwise-elevated proviral loads in orally HTLV-1-infected rats could be reduced by restoration of HTLV-1-specific T-cell responses.[30,31] Furthermore, DNA vaccines or peptide vaccines targeting Tax, the major target antigen recognized by HTLV-1-specific T-cells, can induce antitumor immunity and eradicate HTLV-1-infected lymphomas.[32,33] These observations imply that antitumor therapeutic vaccines targeting Tax might be promising.

It is important to clarify the immunological status of ACs, since insufficiency in host T-cell responses against HTLV-1 could be an immunological risk factor for ATL. HTLV-1-specific CTL responses are also detectable in ACs.[34,35] However, because a wide survey for HTLV-1-specific T-cell immunity has never been carried out, the questions of the proportion of ACs with proper levels of immune responses and the possible existence of a population of ACs with insufficient anti-HTLV-1 responses before ATL onset, remain unresolved. One reason for the poor status of such immunological surveys among ACs is the absence of simple methods for measuring HTLV-1-specific T-cell responses, as they are restricted by individual human leukocyte antigens (HLAs).

We recently established a detection system for HTLV-1-specific T-cell responses using recombinant Tax proteins fused to

[8]To whom correspondence should be addressed. E-mail: kann.impt@tmd.ac.jp

doi: 10.1111/j.1349-7006.2008.01054.x

glutathione-*S*-transferase (GST), in which Tax antigens are processed by antigen-presenting cells and capable of stimulating both $CD4^+$ and $CD8^+$ T-cells among self PBMCs.[36] In this study, by using this assay, we analyzed HTLV-1-specific T-cell responses in unselected ACs and smoldering-type ATL (sATL) patients. We examined sATL samples together because their peripheral lymphocyte numbers are in the normal range (< 4000/μL) and the prognoses vary among individuals.[37,38] Here, we demonstrated wide diversity in T-cell response patterns against HTLV-1 in ACs and sATL patients. Among them, we found some individuals exhibiting impaired Tax-specific T-cell responses associated with poor control of HTLV-1 both in ACs and sATL patients.

Materials and Methods

Subjects. A total of 21 ACs, five HAM/TSP patients, four sATL patients, two chronic-type ATL (cATL) patients, and two acute ATL patients in long-term remission (>2 and >5 years) after allogeneic HSCT donated peripheral blood samples after providing written informed consent. PBMCs were isolated by Ficoll-Paque PLUS (GE Healthcare UK, Buckinghamshire, UK) density gradient centrifugation, and either used immediately or stored frozen in liquid nitrogen in Bambanker stock solution (NIPPON Genetics Co., Tokyo, Japan).

Separation of PBMC fractions. $CD4^+$ or $CD8^+$ cells were depleted from PBMCs by negative selection using 10-fold numbers of Dynabeads M-450 CD4 or CD8 (Dynal Biotec, Oslo, Norway), respectively, according to the manufacturer's instructions. $CCR4^+$ cells were depleted from PBMCs using Dynabeads goat antimouse IgG (Dynal Biotec) following incubation with carboxyfluorescein-conjugated anti-CCR4 monoclonal antibody (mAb) for 45 min at 4°C. The resulting contamination by $CD4^+$, $CD8^+$, or $CCR4^+$ cells was between 0.02% and 3.90% of the total lymphocytes, as analyzed by flow cytometry. The PBMC concentrations were adjusted to 1×10^6 cells/mL before depletion, and the resulting $CD4^+$, $CD8^+$, or $CCR4^+$ cell-depleted fractions were resuspended in medium with the same initial volume, irrespective of the remaining cell numbers.

Recombinant proteins and peptides. GST-fusion proteins of HTLV-1 Tax-A, Tax-B, and Tax-C (corresponding to the N-terminal, central, and C-terminal regions of HTLV-1 Tax, respectively) were prepared as described previously.[36] Briefly, partially overlapping DNA fragments designated Tax-A, Tax-B, and Tax-C were inserted into pGEX-2T (GE Healthcare UK) to express the corresponding proteins fused to GST. DH5α competent cells were transformed with these plasmids, and cultured in 2xYT medium supplemented with ampicillin and isopropyl-β-D-thiogalactopyranoside (IPTG) for protein expression. Individual GST–Tax proteins in inclusion bodies were extracted by sonication and purified using Glutathione Sepharose 4B affinity columns (GE Healthcare UK), followed by size exclusion gel chromatography. The purified proteins were stored at –80°C. The concentrations used were 12.5 μg/mL for GST and 18.75 μg/mL for a mixture of GST–Tax A, B, and C proteins (6.25 μg/mL for each protein). In some experiments, a synthetic peptide corresponding to Tax 301-309 (SFHSLHLLF) and Tax 88-96 (KVLTPPITH), representing the major CTL epitopes restricted by HLA-A24 and A11, respectively, was used as an antigen at 10 μM in PBMC cultures.[29,39]

Assay for T-cell responses. Whole PBMCs (2×10^5 cells/well) or various cell-depleted PBMC fractions starting from the same number of whole PBMCs were incubated with various antigens in 96-well round-bottom culture plates in duplicate wells. The culture medium was RPMI-1640 supplemented with 10% heat-inactivated fetal bovine serum (FBS), 100 U/mL of penicillin, 100 μg/mL of streptomycin, and 2 mg/mL of sodium bicarbonate. To avoid the potential influence of endotoxin contamination of the recombinant proteins, 10 μg/mL of polymyxin B was added to all assays. After 4 days of culture, the supernatants were harvested and stored at –20°C until analysis. The concentrations of interferon (IFN)-γ in the supernatants were measured using a Human IFN-γ ELISA Kit (BioSource, Camarillo, CA, USA) or OptEIA Human IFN-γ ELISA Set (BD Biosciences). The absorbances at 450 nm were measured using a microplate reader and analyzed with the Microplate Manager III software (Bio-Rad Laboratories). In some experiments, a Human Th1/Th2 Cytokine Kit for a Cytokine Beads Assay (CBA) (BD Biosciences) was used to measure various cytokines, including IFN-γ.

Flow cytometry. For cell surface phenotyping, phycoerythrin (PE)-Cy5-conjugated anti-CD4 and PE-Cy5-conjugated anti-CD8 mAbs, carboxyfluorescein-conjugated anti-CCR4 mAb, and appropriate isotype controls were used. Uncultured PBMCs were incubated with these mAbs individually or in combination for 30 min at 4°C, before being washed in phosphate-buffered saline (PBS) containing 1% FBS and fixed with 1% formaldehyde in PBS. For tetramer staining, PBMCs were stained with PE-Cy5-conjugated anti-CD8 mAb for 30 min at 4°C, and then with PE-conjugated HLA-A*1101/Tax88-96, HLA-A*1101/Tax272–280, or HLA-A*2402/Tax301-309 tetramers (National Institute of Allergy and Infectious Diseases Tetramer Facility, Emory University Vaccine Center, Atlanta, GA, USA) for 45 min at 4°C.[29,39] The samples were analyzed using a FACSCalibur and the CellQuest software (BD Biosciences).

HTLV-1 antibody titer. The titers of HTLV-1-specific antibodies in the plasma samples were determined by the particle agglutination method by using Serodia HTLV-1 (FUJIREBIO, Tokyo, Japan) according to the manufacturer's instructions.

HTLV-1 proviral loads. HTLV-1 proviral loads in PBMCs were measured by quantitative real-time polymerase chain reaction (PCR) with HTLV-1 Tax-specific primers through the clinical diagnostic services of SRL Inc. (Tokyo, Japan) or the Group of Joint Study on Predisposing Factors of ATL Development (JSPFAD, Japan) as described previously.[40,41] Proviral DNA copy numbers in various fractions of PBMC samples were measured by SYBR Green quantitative real-time PCR methods using Tax-specific primers (forward: 5′-cggatacccagtctacgtgtttggagactgt-3′, reverse: 5′-gagccgataacgcgtccatcgatggggtcc-3′) and control beta-globin primers (forward: 5′-acacaactgtgttcactagc-3′, reverse: 5′-caacttcatccacgttcacc-3′).

Statistical analysis. The Mann–Whitney *U*-test was used to examine the statistical difference in HTLV-1 proviral loads between two groups by using the Graphpad Prism 4 (Graphpad Software). *P*-values <0.05 were considered significant.

Results

Detection of different patterns of Tax-specific T-cell responses in various diseases associated with HTLV-1 infection. In order to obtain typical patterns of T-cell responses detected by the Tax protein-based assay, we examined PBMCs from HTLV-1-infected patients with various clinical conditions (Fig. 1a). Two ATL patients (#37, #253) who had been in long-term complete remission after HSCT showed clear Tax-specific IFN-γ production, only against GST–Tax protein but not against control GST protein. PBMCs from HAM/TSP patients (#254, #259) produced high levels of IFN-γ in response to GST–Tax, but also in the presence of medium alone or the control GST. In contrast, PBMCs from two cATL patients (#227, #249) showed very weak responses to any stimulation. Although the PBMCs from uninfected individuals showed low levels of background responses that might involve macrophages or natural killer cells, the levels of IFN-γ production in cATL samples were even lower than the background responses.

HTLV-1-infected cells have been reported to express the chemokine receptor CCR4 frequently.[13] As shown in Fig. 1(b),

doi: 10.1111/j.1349-7006.2008.01054.x

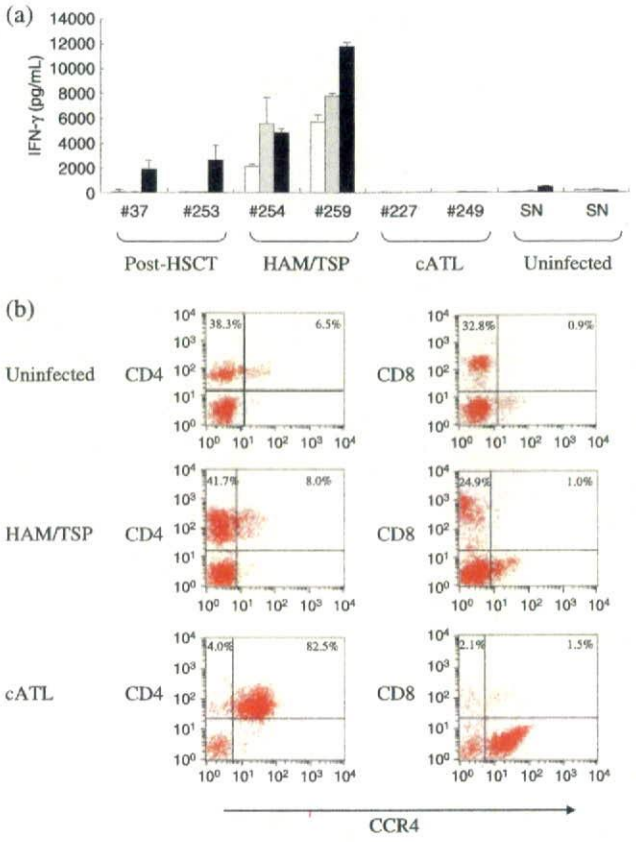

Fig. 1. Different patterns of Tax-specific T-cell responses in various diseases associated with human T-cell leukemia virus type-1 (HTLV-1) infection. (a) Peripheral blood mononuclear cells (PBMCs) (2.0×10^5 cells/well) from two post-hematopoietic stem cell transplantation (HSCT) adult T-cell leukemia (ATL) patients in long-term remission (#37, #253), two HTLV-1-associated myelopathy/tropical spastic paraparesis (HAM/TSP) patients (#254, #259), two chronic-type ATL (cATL) patients (#227, #249), and two seronegative uninfected subjects (SN) were cultured alone (open bars), with glutathione-S-transferase (GST) (gray bars) or with a mixture of GST–Tax proteins (black bars) in a total volume of 200 μL of medium/well for 4 days. Interferon (IFN)-γ in the supernatants was measured by enzyme-linked immunoabsorbent assay. The results represent the mean ± SD of duplicate wells. (b) Uncultured PBMCs from an uninfected subject, a HAM/TSP patient (#255), and a cATL patient (#227) were stained with carboxyfluorescein-conjugated CCR4 monoclonal antibody (mAb) together with phycoerythrin (PE)-Cy5-labeled CD4 (left) or CD8 (right) mAbs. Values indicate the percentages of positive cells in each quadrant analyzed by flow cytometry for a total of 10 000 gated lymphocytes.

PBMCs of an uninfected individual contained 44.8% $CD4^+$ cells and 6.5% $CD4^+CCR4^+$ cells. In the cATL patient (#227), the proportion of $CD4^+CCR4^+$ cells was markedly elevated, consistent with previous reports.[13] PBMCs from this cATL patient contained 86.5% $CD4^+$ cells and 82.5% $CD4^+CCR4^+$ cells. In contrast, the proportion of $CD4^+CCR4^+$ cells in the PBMCs from the HAM/TSP patient (#255) was comparable with that in the uninfected individual.

Since the proportion of HTLV-1-infected cells in the peripheral lymphocytes was elevated in cATL, the poor T-cell responses in these samples may be partly explained by the relative scarcity of normal lymphocytes and antigen presenting cells. Such leukemic PBMCs are not suitable for evaluation with a protein-based assay, and we only used PBMCs with lymphocyte numbers within the normal range hereafter.

Diversity in Tax-specific T-cell responses in ACs and sATL patients. Using the GST–Tax protein-based assay system, we next examined the T-cell responses of 21 ACs and four sATL patients. One of the sATL patients (#213) had polyclonal HTLV-1-infected cells but was categorized as sATL because of the number of abnormal lymphocytes was >5%. The hematologic and virologic profiles of the donors tested are summarized in Table 1. The numbers of peripheral lymphocytes of all ACs and sATL patients were within the normal range.

The IFN-γ production levels by whole PBMCs from the ACs and sATL patients in the absence or presence of GST or GST–Tax proteins are shown in Fig. 2(a). The levels and patterns of IFN-γ production varied widely among individuals. We divided the samples into two groups, according to Tax-specificity of the responses. This was assessed by calculating the ratio of IFN-γ produced in response to GST–Tax proteins divided by IFN-γ produced in response to GST alone for each sample (Tax/GST ratios). Tax-specific patterns were observed in samples from seven ACs (#228, #232, #238, #251, #258, #264, #277) and one sATL patient (#265) who had a localized skin lesion but was without apparent abnormal lymphocytes in the peripheral blood. The remaining samples showed less-specific patterns of IFN-γ production due to increased non-specific IFN-γ production or low IFN-γ production to any stimulation.

We compared the individual proviral loads between the two groups with Tax-specific and less-specific T-cell responses (Fig. 2b,c). The group with clear Tax-specific T-cell response possessed significantly lower proviral loads than the less-specific response group either in the total of ACs and sATL patients ($P = 0.0107$) or in ACs alone ($P = 0.0260$). The three sATL patients (#213, #252, #220) with highest proviral loads among those tested (>100 copies/1000 PBMCs), and several ACs with moderate levels of proviral loads (10–100 copies/1000 PBMCs) were in the less-specific response group. However there were also some ACs who exhibited low T-cell responses and low proviral loads (<10 copies/1000 PBMCs).

Involvement of $CCR4^+$ cells in high background IFN-γ production by PBMCs from HAM/TSP patients. We next assessed what cells in the PBMCs were responsible for the high background IFN-γ production observed in HAM/TSP patients by depleting $CD4^+$, $CD8^+$, or $CCR4^+$ cells from PBMCs prior to the assay. In order to see the effects of cell depletion, the cell concentrations were equalized before cell depletion, and the resulting cell fractions were resuspended in the same volume, irrespective of the final cell numbers. The results are shown in Fig. 3(a). Whole PBMCs from a HAM/TSP patient (#255) showed high levels of non-specific IFN-γ production with or without GST–Tax proteins. When the $CD4^+$ cells were depleted, decreased but significant levels of IFN-γ were only produced in response to GST–Tax proteins. $CD8^+$ cell depletion did not markedly alter the non-specific responses. $CCR4^+$ cell depletion reduced the non-specific responses, but retained Tax-specific IFN-γ production at a level comparable to that of whole PBMCs. These results indicated that $CCR4^+$ PBMC population from this patient mainly contributed to the non-specific responses in the assay, and that the effector of the Tax-specific responses was included in the $CCR4^-$ population that contained $CD4^+$ and $CD8^+$ cells.

We also measured the HTLV-1 p19 levels in the supernatants of these PBMC cultures after 7 days, and found that HTLV-1 p19 became detectable only in the $CD8^+$ cell-depleted fraction but not in the whole or $CD4^+$ cell-depleted or $CCR4^+$ cell-depleted fractions (Fig. 3b). Since the starting PBMC number before cell-depletion in each fraction was equivalent, the increase in p19 production in the $CD8^+$ cell-depleted fraction indicated that $CD8^+$ cells served as suppressors of viral expression in culture.

Reduction in the non-specific IFN-γ production by $CCR4^+$ cell-depletion and enhancement in p19 production by $CD8^+$

Table 1. Blood samples from asymptomatic HTLV-1 carriers (ACs) and smoldering ATL (sATL) patients tested

ID	Age	Sex	Clinical status	WBC/μL	Lymphocyte (%)	Abnormal lymphocyte (%)	Provirus DNA copies/1000 PBMCs	Plasma HTLV-1 antibody titer†
#211	20s	F	AC	4500	34	0	33	>8192
#213	50s	F	sATL‡	7500	36	8	200	4096
#215	20s	M	AC	8000	55	0	13	2048
#216	70s	F	AC	4200	31	3	39	>8192
#217	70s	F	AC	6800	51	0	14	>8192
#218	50s	F	AC	7500	55	0	<1	1024
#219	60s	F	AC	7200	43	0	<1	1024
#220	50s	M	sATL	4800	28	13	277	>8192
#223	60s	M	AC	4200	26	0	<1	1024
#226	50s	M	AC	5700	38	0	28	2048
#228	60s	M	AC	5900	59	0	<1	256
#232	30s	F	AC	5800	46	0	<1	>8192
#236	30s	F	AC	6500	39	0	22	>8192
#238	60s	F	AC	5700	51	0	2	1024
#243	50s	F	AC	4100	58	0	3	2048
#244	50s	F	AC	4900	27	3	63	1024
#245	40s	F	AC	5000	46	1	58	1024
#246	50s	M	AC	4600	37	0	2	>8192
#251	60s	M	AC	4800	50	0	2	2048
#252	50s	F	sATL	4100	38	11	207	>8192
#258	60s	M	AC	6400	30	3	8	256
#263	60s	M	AC	3900	49	2	1	2048
#264	50s	F	AC	3000	37	0	<1	256
#265	60s	F	sATL§	4700	38	1	2	2048
#277	50s	F	AC	4100	29	0	<1	256

†Measured by a particle agglutination method.
‡Diagnosed as sATL because of increased abnormal lymphocyte number, although the infected cells were polyclonal.
§Diagnosed as sATL because of the presence of skin lesions.
HTLV-1, human T-cell leukemia virus type-1; ACs, asymptomatic HTLV-1 carriers; ATL, adult T-cell leukemia; sATL, smoldering-type ATL; PMBC, peripheral blood mononuclear cell; WBC, white blood cell.

cell-depletion were also observed in the samples from two other HAM/TSP patients (#288 and #290) (Fig. 3c,d).

The prevalence of HTLV-1-infected cells in the $CCR4^+$ cell fraction was further confirmed by a real-time PCR method in uncultured PBMCs from subjects #255 (HAM/TSP) and #211 (AC), although there were still detectable levels of proviruses left in the $CCR4^+$ cell-depleted fractions (Fig. 3e).

Poor effects of $CCR4^+$ cell depletion on Tax-specific T-cell responses in PBMC cultures from some ACs and sATL patients. We then assessed whether ACs and sATL samples with apparently less-specific responses actually possessed Tax-specific responses, similarly to the samples from HAM/TSP patients. We examined the effects of $CCR4^+$ cell-depletion on Tax-specific T-cell responses and the effects of $CD8^+$ cell-depletion on HTLV-1 p19 production in the PBMC samples from several available ACs and sATL patients with less-specific responses and elevated proviral loads (Fig. 4).

PBMCs from AC #238 were examined as a control that exhibited clear Tax-specific T-cell responses. As shown in Fig. 4, the Tax-specific pattern in this sample was not altered by $CCR4^+$ cell depletion. HTLV-1 p19 production in the PBMC culture of #238 was very low, consistent with the low proviral load in this subject.

In the sample from AC #211, which had a moderately elevated level of proviral load (10–100 copies/1000 PBMCs), whole PBMCs showed a less-specific response pattern with high background IFN-γ production. This was improved to a Tax-specific pattern by depletion of $CCR4^+$ cells. HTLV-1 p19 production in $CD8^+$ cell-depleted fraction from this subject was 10 times higher than that in whole PBMCs, indicating that $CD8^+$ cells efficiently suppressed HTLV-1 p19 production in culture.

The whole PBMCs from AC #244, possessing a proviral load similar to that of subject #211, also showed a less-specific response pattern. $CCR4^+$ cell depletion reduced spontaneous IFN-γ production but did not improve the difference between the responses to control GST and GST–Tax by much. Whole PBMCs from subject #244 spontaneously produced a substantial amount of HTLV-1 p19, which was slightly enhanced by depletion of $CD8^+$ cells.

PBMCs from sATL patient #213, who had a high proviral load (>100 copies/1000 PBMCs), spontaneously produced significant levels of IFN-γ irrespective of the stimulation. Depletion of $CCR4^+$ cells slightly reduced the general levels of IFN-γ production, but did not improve the non-specific pattern. Unfractionated PBMCs from this subject produced high levels of HTLV-1 p19, and $CD8^+$ cell depletion did not alter the levels of HTLV-1 p19 at all.

PBMCs from sATL patient #252, who also had a high proviral load, showed very low levels of IFN-γ production in response to GST or GST–Tax proteins. $CCR4^+$ cell depletion from these PBMCs did not improve the scale or specificity of the IFN-γ production by these PBMCs. Whole PBMCs from subject #252 spontaneously produced a significant amount of HTLV-1 p19, which was slightly increased by $CD8^+$ cell depletion.

Thus, $CCR4^+$ cell depletion revealed Tax-specific T-cell responses in some, but not all, samples with less-specific responses. Samples that did not show a Tax-specific pattern after $CCR4^+$ cell depletion were associated with insufficient control of HTLV-1 production in culture.

Unresponsiveness of Tax-specific CTLs in PBMCs from an AC. Finally, we investigated whether the five subjects shown in Fig. 4 had Tax-specific CTLs, using a flow cytometric analysis with tetramers. As shown in Fig. 5(a), the PBMCs from AC #238 contained HLA-A*1101/Tax88-96 tetramer-binding CTLs,

doi: 10.1111/j.1349-7006.2008.01054.x

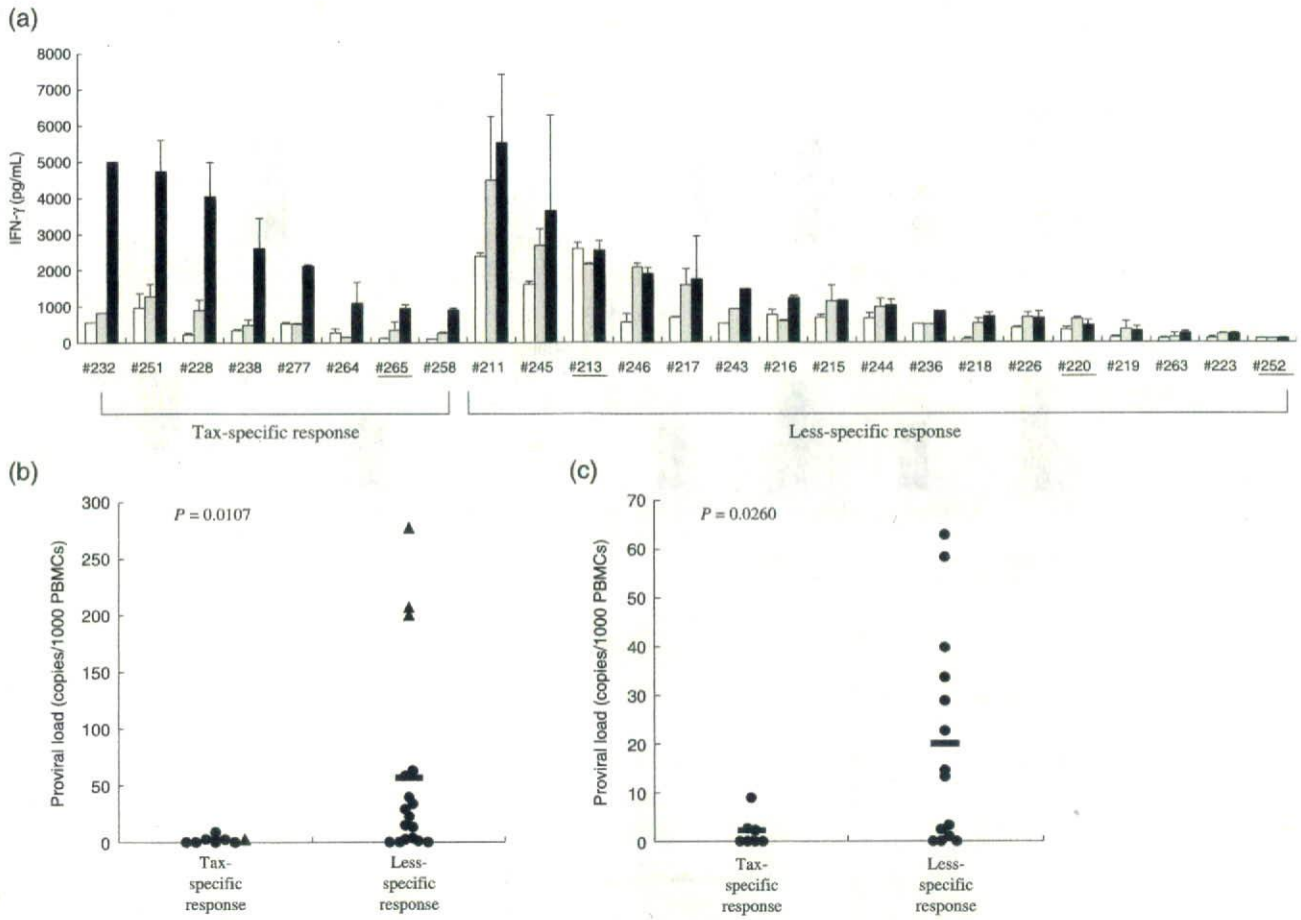

Fig. 2. Diversity in Tax-specific T-cell responses among asymptomatic human T-cell leukemia virus type-1 (HTLV-1) carriers (ACs) and smoldering-type adult T-cell leukemia (sATL) patients. (a) Peripheral blood mononuclear cells (PBMCs) isolated from 21 ACs and 4 sATL patients (underline) were incubated alone (open bars), with glutathione-*S*-transferase (GST) (gray bars) or with a mixture of GST–Tax proteins (black bars) for 4 days, and interferon (IFN)-γ amounts in the supernatants were measured by enzyme-linked immunoabsorbent assay and a Cytokine Beads Assay in part. The results were divided into Tax-specific or less-specific response groups depending on the ratios of anti-GST–Tax/anti-GST IFN-γ production were more than 2.5 or not, and then aligned in the order of absolute values of IFN-γ production against GST–Tax proteins in each group. (b, c) HTLV-1 proviral loads of all the ACs and sATL patients tested (b) or ACs alone (c) were indicated. The mean values of proviral loads (bars) in Tax-specific and less-specific response groups were 2.0 and 56.9 copies/1000 PBMCs, respectively ($P = 0.0107$) in (b), and 1.9 and 20.1 copies/1000 PBMCs, respectively ($P = 0.0260$) in (c). AC, closed circle; sATL: closed triangle.

and ACs #211 and #244 were positive for HLA-A*2402/Tax301-309 tetramer-binding CTLs. In the PBMCs from subjects #213 and #252 (sATL), tetramer-binding cells were not detectable, although these subjects were positive for HLA-A24 and A11, and HLA-A11, respectively (data not shown).

We examined the activity of Tax-specific CTLs by stimulating $CCR4^+$ cell-depleted PBMCs from three ACs, which contained tetramer-binding CTLs, with oligopeptides corresponding to the tetramers in culture. As shown in Fig. 5(b), $CCR4^+$ cell-depleted PBMCs from subjects #238 and #211 produced IFN-γ in response to Tax88-96 and Tax301-309 peptides, respectively, whereas those from subject #244 did not respond to Tax 301-309 peptides. These results are consistent with the results of the assay using GST–Tax proteins and suggest that Tax-specific CTLs in subject #244 might be in an anergic state.

Discussion

In the present study, we investigated HTLV-1-specific T-cell responses in unselected HTLV-1-infected individuals without any bias of HLAs by using a GST–Tax protein-based assay system. This assay detected clear Tax-specific responses in ATL patients in complete remission, less-specific responses in HAM/TSP patients, and very weak responses in cATL patients. Interestingly, all of these patterns were observed in PBMCs from ACs and sATL patients, indicating wide diversity in Tax-specific T-cell responsiveness at these stages. Most importantly, some individuals at these stages exhibited impaired Tax-specific T-cell responses and elevated proviral loads, indicating that such conditions are present before an overt leukemia stage.

High background responses have been an obstacle to evaluate T-cell responses in HTLV-1-infected individuals. This may be similar to the phenomenon known as 'spontaneous proliferation' of PBMCs from HAM/TSP patients and ACs.[42–44] In our study, depletion of $CCR4^+$ cells containing HTLV-1-infected cells from the PBMCs reduced this spontaneous response and revealed a Tax-specific T-cell response pattern in the samples from several HAM/TSP patients and ACs with strong non-specific responses (Figs 3 and 4). The sources of spontaneous IFN-γ production may be either HTLV-1-specific T-cells reacting with coexisting infected cells in culture, or HTLV-1-infected cells themselves, or both.[45,46] As $CCR4^+$ cell depletion from the PBMCs reduced the

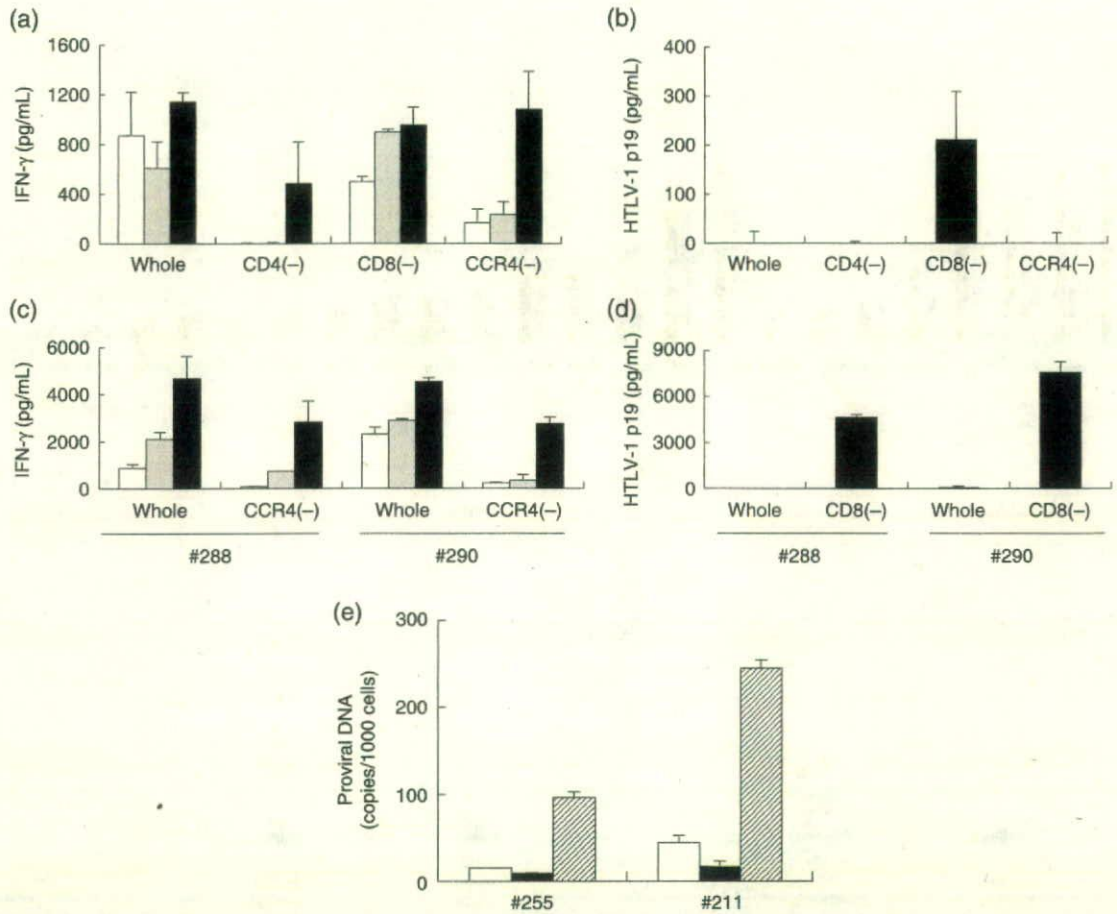

Fig. 3. Involvement of CCR4⁺ cells in high background interferon (IFN)-γ production by peripheral blood mononuclear cells (PBMCs) from human T-cell leukemia virus type-1 (HTLV-1)–associated myelopathy/tropical spastic paraparesis (HAM/TSP) patients. PBMCs from a HAM/TSP patient (#255) were equally divided into four fractions. One fraction was used directly (whole) and the other three fractions were used after depletion of CD4⁺ [CD4(–)], CD8⁺ [CD8(–)], or CCR4⁺ [CCR4(–)] cells. The cell numbers in each fraction were 2.0×10^5, 0.8×10^5, 1.1×10^5, and 1.3×10^5 cells/well, respectively. (a) The fractions were cultured alone (open bars), with glutathione-*S*-transferase (GST) (gray bars), or with a mixture of GST–Tax proteins (black bars) for 4 days. IFN-γ in the supernatants was measured by enzyme-linked immunoabsorbent assay (ELISA). (b) The levels of HTLV-1 p19 antigen in the culture supernatants of the PBMC fractions in the absence of any stimulation were measured by ELISA at 7 days after the initiation of culture. The results represent the mean ± SD of duplicate wells. (c, d) Whole and fractionated PBMCs from two other HAM/TSP patients (#288 and #290) were similarly examined for IFN-γ production for 4 days against medium (open bars), GST (gray bars), or GST–Tax proteins (black bars) (c), and HTLV-1 p19 production for 7 days of culture (d). The cell numbers of whole, CCR4(–), and CD8(–) PBMCs in each well were 2.0×10^5, 1.7×10^5, and 1.2×10^5 for patient #288, and 2.1×10^5, 0.9×10^5, and 0.9×10^5 for patient #290, respectively. (e) HTLV-1 provirus numbers (copies/1000 cells) in whole (open bars), CCR4⁺ cell-depleted (closed bars), and CCR4⁺ (hatched bars) PBMC fractions before culture from subjects #255 (HAM/TSP) and #211 (AC) were measured by real-time polymerase chain reaction methods. The results represent the mean ± SD of duplicate samples.

number of HTLV-1-infected cells without losing CD8⁺ cells, T-cell response against exogenously added Tax proteins became clearly detectable. CD8⁺ cells in these PBMCs effectively suppressed HTLV-1 p19 production in culture, presumably by killing infected cells.

Although the number of samples available for detailed analysis was limited, PBMCs from at least two sATL patients (#213 and #252) with high proviral loads (>100 copies/1000 cells) exhibited impaired T-cell responses even after CCR4⁺ cell depletion. CD8⁺ cells of these subjects had poor effects on HTLV-1 p19 production (Fig. 4). This was not attributable to the scarcity of non-ATL cells, as these PBMCs contained 16.5% and 12.0% CD8⁺ cells, respectively. HTLV-1-infected cells were the most likely source of IFN-γ production in whole and CCR4⁻ PBMC cultures from subject #213, as HTLV-1 p19 was detected even in the CCR4⁺ cell-depleted fraction during further culture (data not shown), presumably because of expansion of the remaining infected cells in the initially CCR4⁻ cell culture, in the absence of any anti-Tax response. HTLV-1-infected cells from subject #252 expressed viral antigens but not IFN-γ.

ACs with less-specific T-cell responses and moderate levels of proviral loads (10–100 copies/1000 PBMCs) seemed to be a mixed population in regards to Tax-specific response. CCR4⁺ cell-depleted PBMCs showed Tax-specific T-cell response in subject #211, but did not markedly do so in subject #244. Similarly, CD8⁺ cell-mediated control on HTLV-1 p19 production in #211 was more efficient than in #244. The results of peptide stimulation also indicated impaired status of Tax-specific response in #244 (Figs 4 and 5). However, the level of p19 production in the CD8⁺ cell-depleted cell fraction was even higher

doi: 10.1111/j.1349-7006.2008.01054.x

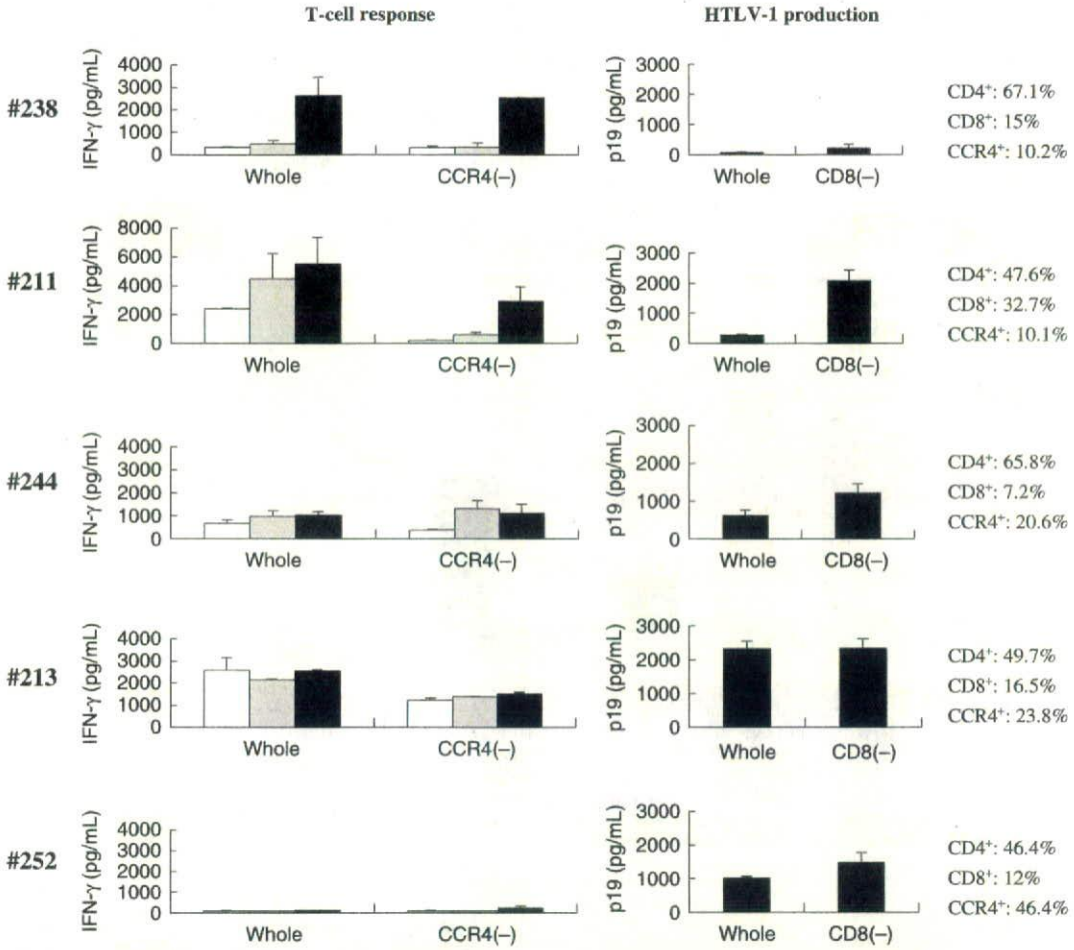

Fig. 4. Tax-specific T-cell response associated with CD8⁺ cell-mediated control of human T-cell leukemia virus type-1 (HTLV-1) production in peripheral blood mononuclear cell (PBMC) cultures from asymptomatic HTLV-1 carriers (ACs) and smoldering-type adult T-cell leukemia (sATL) patients. Whole and CCR4⁺ cell-depleted [CCR4(–)] PBMC fractions prepared from subjects #238 (AC), #211 (AC), #244 (AC), #213 (sATL), and #252 (sATL) were cultured alone (open bars), with glutathione-*S*-transferase (GST) (gray bars), or with a mixture of GST–Tax proteins (black bars) for 4 days. Interferon (IFN)-γ produced in the supernatants was measured by enzyme-linked immunoabsorbent assay (left panels). The levels of HTLV-1 p19 production in whole and CD8⁺ cell-depleted [CD8(–)] PBMC cultures from the same donors were measured on day 7 (right panels). The ratios of CD4⁺, CD8⁺, and CCR4⁺ cells (%) in uncultured PBMCs from each subject were indicated at right, as determined by flow cytometry.

in #211. Nevertheless, #211 and #244 had comparable levels of proviral loads (33 and 63 copies/1000 PBMCs, respectively). These results suggested that proviral load might represent equilibrium between growth capabilities of infected cells and the T-cell response against them.

It is of note that some ACs (#219, #223, #263) exhibited very low anti-Tax T-cell responses that were not improved by CCR4⁺ cell depletion, and also had low proviral load. HTLV-1-infected cells in these individuals might have low proliferative abilities. Since these subjects maintained considerable levels of anti-HTLV-1 antibodies in the plasma (1:1024–2048, Table 1), poor T-cell responsiveness cannot be explained merely by the scarcity of viral antigens. The mechanisms of general and/or HTLV-1-specific immune suppression in HTLV-1 infection remain to be clarified.

In conclusion, ACs and sATL patients consist of diverse subpopulations with different patterns of T-cell responses against HTLV-1, containing a subpopulation exhibiting impaired HTLV-1-specific T-cell responses and insufficient control of HTLV-1-infected cells. This strongly suggests that impairment of HTLV-1-specific T-cell response is not a consequence of advanced ATL but present at early stages or even before the disease onset. Although there must be multiple steps towards ATL development, impaired HTLV-1-specific T-cell response could be one of the underlying conditions that allows expansion of HTLV-1 infected cells *in vivo*. Reactivation of HTLV-1-specific T-cell response by immunotherapeutic strategies such as vaccines in the subpopulation with insufficient T-cell response might contribute to the recovery of host control on HTLV-1-infected cells *in vivo*.

Acknowledgments

We thank Ms. Minako Nakashima and Ms. Yasuko Tsuji (Imamura Bun-in Hospital, Kagoshima, Japan) for coordination of clinical samples. This study was supported by Grant 17013028 from the Ministry of Education, Culture, Sports, Science, and Technology of Japan; a grant for an anticancer project from the Ministry of Health, Welfare, and Labor of Japan; and the Public Trust Haraguchi Memorial Cancer Research Fund. The authors have no financial conflict of interest.

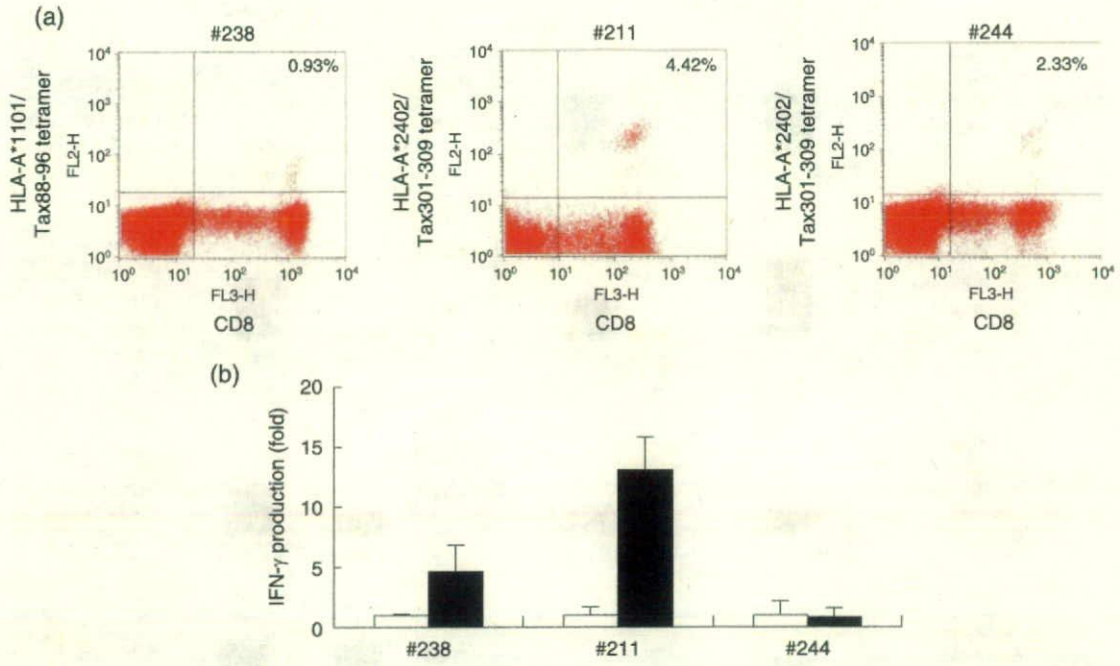

Fig. 5. Discrepancy between the presence of Tax-specific cytotoxic T-lymphocytes (CTLs) and interferon (IFN)-γ production in peripheral blood mononuclear cells (PBMCs) from asymptomatic human T-cell leukemia virus type-1 (HTLV-1) carriers (ACs). (a) Uncultured PBMCs from indicated subjects were stained with phycoerythrin (PE)-Cy5-conjugated CD8 monoclonal antibody (mAb) together with PE-conjugated HLA-A*1101/Tax88-96 tetramers for subject #238, and HLA-A*2402/Tax301-309 tetramers for subjects #211 and #244. The percentages of tetramer$^+$ cells among CD8$^+$ cells are indicated, as analyzed by flow cytometry. (b) CCR4$^+$ cell-depleted PBMCs from the same subjects were incubated with control dimethylsulfoxide (DMSO) (open bars) or 10 μM of Tax peptides (closed bars) for 4 days, and the amounts of IFN-γ in the supernatants were measured by enzyme-linked immunoabsorbent assay. Tax peptides used were Tax 88-96 for subject #238 and Tax 301-309 for subjects #211 and #244. The values represent folds of IFN-γ production against control DMSO, and indicated as the mean ± SD of duplicate samples.

References

1 Hinuma Y, Nagata K, Hanaoka M *et al.* Adult T-cell leukemia: antigen in an ATL cell line and detection of antibodies to the antigen in human sera. *Proc Natl Acad Sci USA* 1981; **78**: 6476–80.

2 Poiesz BJ, Ruscetti FW, Gazdar AF, Bunn PA, Minna JD, Gallo RC. Detection and isolation of type C retrovirus particles from fresh and cultured lymphocytes of a patient with cutaneous T-cell lymphoma. *Proc Natl Acad Sci USA* 1980; **77**: 7415–19.

3 Uchiyama T, Yodoi J, Sagawa K, Takatsuki K, Uchino H. Adult T-cell leukemia: clinical and hematologic features of 16 cases. *Blood* 1977; **50**: 481–92.

4 Tajima K. The 4th nation-wide study of adult T-cell leukemia/lymphoma (ATL) in Japan: estimates of risk of ATL and its geographical and clinical features. The T- and B-cell Malignancy Study Group. *Int J Cancer* 1990; **45**: 237–43.

5 Arisawa K, Soda M, Endo S *et al.* Evaluation of adult T-cell leukemia/lymphoma incidence and its impact on non-Hodgkin lymphoma incidence in southwestern Japan. *Int J Cancer* 2000; **85**: 319–24.

6 Gessain A, Barin F, Vernant JC *et al.* Antibodies to human T-lymphotropic virus type-I in patients with tropical spastic paraparesis. *Lancet* 1985; **2**: 407–10.

7 Osame M, Usuku K, Izumo S *et al.* HTLV-1 associated myelopathy, a new clinical entity. *Lancet* 1986; **1**: 1031–2.

8 Hisada M, Okayama A, Spiegelman D, Mueller NE, Stuver SO. Sex-specific mortality from adult T-cell leukemia among carriers of human T-lymphotropic virus type I. *Int J Cancer* 2001; **91**: 497–9.

9 Hisada M, Okayama A, Tachibana N *et al.* Predictors of level of circulating abnormal lymphocytes among human T-lymphotropic virus type I carriers in Japan. *Int J Cancer* 1998; **77**: 188–92.

10 Okayama A, Stuver S, Matsuoka M *et al.* Role of HTLV-1 proviral DNA load and clonality in the development of adult T-cell leukemia/lymphoma in asymptomatic carriers. *Int J Cancer* 2004; **110**: 621–5.

11 Nagai M, Usuku K, Matsumoto W *et al.* Analysis of HTLV-1 proviral load in 202 HAM/TSP patients and 243 asymptomatic HTLV-1 carriers: high proviral load strongly predisposes to HAM/TSP. *J Neurovirol* 1998; **4**: 586–93.

12 Ishida T, Utsunomiya A, Iida S *et al.* Clinical significance of CCR4 expression in adult T-cell leukemia/lymphoma: its close association with skin involvement and unfavorable outcome. *Clin Cancer Res* 2003; **9**: 3625–34.

13 Yoshie O, Fujisawa R, Nakayama T *et al.* Frequent expression of CCR4 in adult T-cell leukemia and human T-cell leukemia virus type 1-transformed T cells. *Blood* 2002; **99**: 1505–11.

14 Karube K, Ohshima K, Tsuchiya T *et al.* Expression of FoxP3, a key molecule in CD4CD25 regulatory T cells, in adult T-cell leukaemia/lymphoma cells. *Br J Haematol* 2004; **126**: 81–4.

15 Matsubara Y, Hori T, Morita R, Sakaguchi S, Uchiyama T. Phenotypic and functional relationship between adult T-cell leukemia cells and regulatory T cells. *Leukemia* 2005; **19**: 482–3.

16 Kohno T, Yamada Y, Akamatsu N *et al.* Possible origin of adult T-cell leukemia/lymphoma cells from human T lymphotropic virus type-1-infected regulatory T cells. *Cancer Sci* 2005; **96**: 527–33.

17 Sakaguchi S, Sakaguchi N, Shimizu J *et al.* Immunologic tolerance maintained by CD25$^+$ CD4$^+$ regulatory T cells: their common role in controlling autoimmunity, tumor immunity, and transplantation tolerance. *Immunol Rev* 2001; **182**: 18–32.

18 Sebastiani S, Allavena P, Albanesi C *et al.* Chemokine receptor expression and function in CD4$^+$ T lymphocytes with regulatory activity. *J Immunol* 2001; **166**: 996–1002.

19 Iellem A, Mariani M, Lang R *et al.* Unique chemotactic response profile and specific expression of chemokine receptors CCR4 and CCR8 by CD4 (+) CD25 (+) regulatory T cells. *J Exp Med* 2001; **194**: 847–53.

20 Shevach EM. CD4$^+$ CD25$^+$ suppressor T cells: more questions than answers. *Nat Rev Immunol* 2002; **2**: 389–400.

21 Chen S, Ishii N, Ine S *et al.* Regulatory T cell-like activity of Foxp3$^+$ adult T cell leukemia cells. *Int Immunol* 2006; **18**: 269–77.

22 Katsuki T, Katsuki K, Imai J, Hinuma Y. Immune suppression in healthy carriers of adult T-cell leukemia retrovirus (HTLV-1). impairment of T-cell control of Epstein-Barr virus-infected B-cells. *Jpn J Cancer Res* 1987; **78**: 639–42.

23 Nakada K, Yamaguchi K, Furugen S *et al.* Monoclonal integration of HTLV-1 proviral DNA in patients with strongyloidiasis. *Int J Cancer* 1987; **40**: 145–8.

doi: 10.1111/j.1349-7006.2008.01054.x